Foundations of Molecular Electronics – Charge Transport in Molecular Conduction Junctions

Joshua Jortner[1], Abraham Nitzan[1] and Mark A. Ratner[2]

[1] School of Chemistry, Tel Aviv University, Tel Aviv, 69978, Israel
[2] Department of Chemistry and Institute for Nanotechnology, Northwestern University, Evanston, Illinois 60208, U.S.A.

Abstract. The most fundamental structure involved in molecular electronics is a molecular transport junction, consisting of one (ideally) or more molecules extending between two electrodes. These junctions combine the fundamental process of intramolecular electron transfer with the mixing of molecular and continuum levels at the electrodes and the nonequilibrium process of voltage-driven currents. Much of this book is devoted to the complicated but significant behaviors that arise from this conjunction. This introductory chapter attempts to sketch some of the principles and also some of the unresolved issues that characterize molecular transport junctions.

Sections 2–4 deal with fundamental ideas. These include an appropriate theoretical formulation of the conductance calculation in terms of non-equilibrium Green's functions, the relationship between junction conductance and nonadiabatic electron transfer rates in the same molecular entities, and the role and magnitude of interactions between the dynamics of the transferring electronic charges and the nuclear degrees of freedom. Section 5 addresses some of the outstanding and difficult issues in understanding junction transport, including geometry and its change with voltage, the electrostatic profile under applied voltage, electronic structure models and their limitations, and fluctuations and switching phenomena in junctions.

Molecular electronics is an area of very rapidly growing scientific and applied interest and activity. While the technological drivers, including materials, electrochemical, biological, sensing, memory and logic applications are all important, the fundamental issues involved in the nonequilibrium responses of molecule-based hybrid materials to applied electromagnetic fields is the fundamental driver for this science. In this sense, molecular electronics is a sort of spectroscopy. Due to the intensity and quality of the research being done in the area, the community may soon be able to understand molecular transport spectroscopy at a level of depth and sophistication almost comparable to other, more traditional spectroscopies. Contemporary research in the area, as exemplified in this book and at the Dresden conference that initiated the book, is driving in that direction.

1 Prologue

Molecular electronics, one of the major fields of current efforts in nanoscience, involves the exploration of the electronic level structure, response and transport, together with the development of electronic devices and applications that depend on the properties of matter at the molecular scale. This includes

single molecules, molecular arrays and molecular networks connected to other electronic components. Its major application areas include sensors, displays, smart materials, molecular motors, logic and memory devices, molecular scale transistors and energy transduction devices. Often molecular electronics is envisioned as the next step in device miniaturization. The importance of molecules in device applications stems not only from their electronic properties, but also from their ability to bind to one another, recognize each other, assemble into larger structures, and exhibit dynamical stereochemistry [1–11].

While the promise of new technological breakthroughs has been a major driving force in this field, consideration of molecular systems as components of electronic devices raises important fundamental questions. In particular, while traditional quantum chemistry deals with molecules as electronically closed systems, practitioners of molecular electronics face problems involving molecular systems that are open to their electronic environment and, moreover, function in situations far from equilibrium. Informed design of such devices requires an understanding of the interplay among molecular structure, dynamics and function. In addition, for particular applications such as switching, rectification and memory storage/reading on the molecular level, we need to understand the non-linear response of such systems. Possible heating in such junctions should be considered as well, implying the need to understand relaxation and heat conduction in such molecular structures. Finally, the vision to adjust and to monitor the operation of these devices brings out the need to understand different control modes, ranging from structural design to interaction with external forces such as a radiation field or other molecular entities.

During the past half century remarkable progress was made in establishing the conceptual framework for electron transfer (ET) processes [11] in molecular, supermolecular, and biophysical systems. ET provides a central conceptual and technical basis for molecular electronics, pertaining both to molecular devices and to molecular materials. ET in supermolecules falls into two general categories: (1) Bridged species, often consisting of an electron donor (D) and an electron acceptor (A), linked by a non-rigid or a rigid molecular bridge (B); and (2) biophysical systems such as the photosynthetic reaction centers (RC) of bacteria and plants, where the primary process (the conversion of solar energy into chemical energy) proceeds via a sequence of well-organized, highly efficient, directional and specific ET processes between prosthetic groups embedded in the protein medium.

The control of ET in donor/bridge/acceptor (DBA) or donor/acceptor (DA) systems in solution [12], in a solid [13], in a protein [14], in DNA [15] or within an "isolated" solvent-free supermolecule [16] can be accomplished by: (1) Structural control. 'Molecular engineering' of the D, A and B subunits determines the molecular energetics and the direct D–A or superexchange D–B–A electronic coupling. (2) Intramolecular dynamic control of the nuclear equilibrium configurational changes (i.e. nuclear distortions) that accompany

ET [17]. (3) Medium control of 'conventional' ET in a solvent or in a cluster. The functions of the medium on DBA $\rightarrow$ D^+BA^- ET include: (i) the energetic stabilization of the ionic states; (ii) and the coupling of the electronic states with the medium nuclear motion, which originates from short-range and long-range interactions in polar solvents, with short-range interactions with C–H group dipoles in non-polar hydrocarbons and with polar amino acid residues in protein. (4) Dynamic medium control of ET [18] involving either the medium acting as a heat bath, solvent-controlled ET, specific dynamic control of pathways by solvent motions ('gating'), or very slow solvent relaxations such as in glassy matrices, that lead to reduced solvent reorganization energies.

The structural, intramolecular, solvent, and dynamic control of ET allows for the design of molecular systems where ET is: (i) ultrafast (on the time scale of $\sim$1 ps to $\sim$100 fs), overwhelming any energy waste processes; (ii) highly efficient, eliminating any back reactions; (iii) stable with respect to the predictable variation of molecular and medium properties; (iv) practically invariant with respect to temperature changes.

ET theory for donor–acceptor charge transfer represents the non-adiabatic ET rate $k_{\mathrm{D}\rightarrow\mathrm{A}}$ in the basic form

$$k_{\mathrm{D-A}} = (2\pi/\hbar)V^2\mathcal{F} \tag{1}$$

where V is the effective electronic coupling and $\mathcal{F}$ is the thermally averaged nuclear vibrational Franck-Condon factor. This microscopic description rests on several ingredients: (1). ET is described as a radiationless transition. (2). The Born-Oppenheimer separability of electronic and nuclear motion applies, enabling the description of the system in terms of diabatic potential surfaces Fig. 1 (3). The electronic coupling is sufficiently weak to warrant the description of the radiationless transition in the non-adiabatic limit. (4). Microscopic ET rates are insensitive to medium dynamics. This state of affairs is realized for the common situation of clear separation of time scales between electronic and nuclear processes. (5). Incoherent charge transfer between the donor-acceptor sites, involving dephasing at each ET step. This state of affairs is analogous to Holstein's small polaron [19] in the incoherent limit.

The electronic coupling in the DBA system $V = V_{\mathrm{DA}} + V_{\mathrm{super}}$ consists of a sum of a direct D–A exchange contribution V_{DA} between the electronic states of DA and D^+A^-, and a superexchange off-resonance interaction [20] V_{super}. The accumulated information concerning the distance dependence of both direct and superexchange interactions is that both interactions are expected to exhibit an exponential distance dependence [21]

$$V = \alpha\, \exp(-\beta R_{\mathrm{DA}})\,, \tag{2}$$

where R_{DA} is the (either edge-to-edge or center-to-center) D–A distance. The distance dependence of intramolecular superexchange interactions in man-made synthetic systems and nature-made biological photosynthetic systems

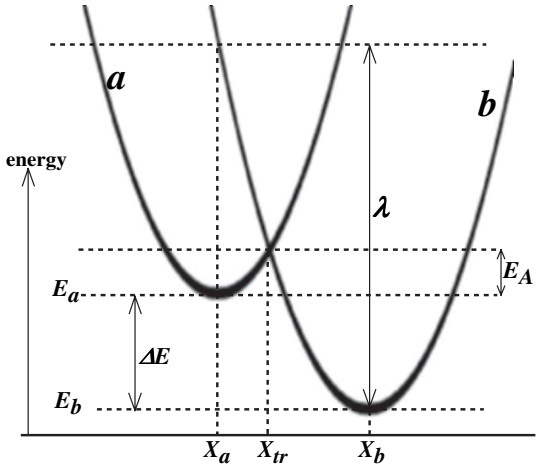

Fig. 1. A schematic diagram showing the energetics of an electron transfer reaction in terms of two diabatic surfaces, characterized by their curvature, the gap energy ΔE and the reorganization energy λ

and in DNA provides a dynamic ruler for the interrogation of the distance dependence of incoherent charge transfer between molecular sites, which are driven by the electronic coupling with $k_{\mathrm{D}\to\mathrm{A}}$ constrained by the nuclear Franck-Condon factor.

In direct comparison with the ET picture in Fig. 1, the simplest energy representation for a molecular transport junction (MJ) is given in Fig. 2. The two electrodes are assumed made of the same material, which is taken to be simple metal with a Fermi level denoted E_f. The discrete levels shown for the molecule represent (just as the continuum levels in the metal do) one-electron energies. In particular, the highest-occupied and lowest empty molecular orbitals (HOMO and LUMO respectively) define a gap, and E_f must lie within this gap. Under conditions where these metals are thermally equilibrated, the Landauer formula for the coherent conductance of the junction is given by (1)

$$g(\Phi) = \frac{e}{\pi\hbar}\frac{\partial}{\partial\Phi}\int_0^\infty dE\mathcal{T}(E)\left(f(E) - f(E + e\,\Phi)\right) \tag{3}$$

(here $g, \Phi, \mathrm{T}, f, E$, are respectively the conductance, the voltage, the transmission through the molecular junction, the Fermi functions describing the populations on the two metal leads and the energy variable). When the derivative on the rhs of (3) is removed, one obtains a formula for the current, I, in terms of the populations and the elastically-scattered transmission. Equation (3) is the simplest useful result for transport, and has the same role there that (1) has in the ET processes. It is actually reminiscent of the ET result of (1): the rate (ET) or the current (molecular junctions) is given by the product of a population term and a scattering probability.

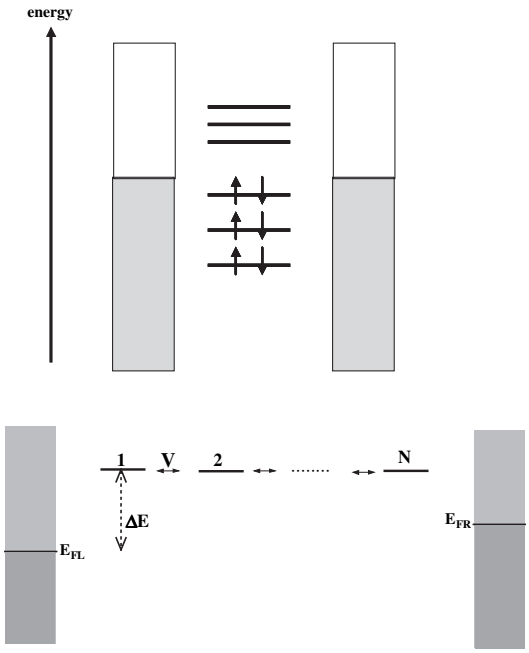

Fig. 2. (**a**) A schematic diagram of a molecular junction, comprising two electrodes with Fermi energies E_{FL} and $E_{FR}(E_{FR} - E_{FL} = e\Phi)$ connected by a molecular species. The latter is characterized by its HOMO-LUMO gap, as shown. (**b**) Same as (a), except that the molecule is represented in a local (e.g. atomic orbital) basis set

As a voltage is applied to the junction, the two Fermi levels differ by Φe, the voltage times the elementary charge. Whenever one of the Fermi levels crosses a molecular level, there is a possibility for resonant transfer, and one expects a local maximum in the $g(\Phi)$ measurement.

The similarity of the rate measurement in nonadiabatic intramolecular ET and the transport in molecular junctions is striking. The comparison is made explicit in Table 1.

Table 1. Comparison of Rate and Transport Processes

Intramolecular Nonadiabatic Rates	Molecular Junction Transport
rate constant $k(\sec^{-1})$	conductance $g(\Omega^{-1})$
electron tunneling	electron tunneling
vibronic bath	electronic bath (electrodes)
(1)	(3)

Since both processes are determined by electron tunneling, they are closely related to one another, as will be discussed in Sect. 3, after a brief description of conductance formulations in Sect. 2. The bath medium, into which the energy is dissipated, differs from the vibrations and solvent polarization in ET to the electrode Fermi sea for simple coherent transport in junctions; this leads to quite different temperature dependences for the two phenomena.

Section 3 discusses the magnitudes expected for the conductance and for the rate constants, and presents an analysis of the relationship between these two important observable properties. Section 4 is devoted to behaviors arising from the interactions of the electronic and vibrational degrees of freedom, including inelastic tunneling spectroscopy and the transition from coherent to activated behavior. Section 5 presents a very brief overview of some of the outstanding issues involved in modeling transport junctions.

Over the past half century the properties of non-molecular electronic materials, i.e., metals, semiconductors and dielectrics, and their interfaces, have been investigated extensively and are well understood. Only relatively recently was a similar effort directed towards systems involving molecular, mostly organic, materials. During the past decade a new focus on the electronic transport properties of single molecule junctions, as well as molecular and biomolecular DNA chains, is emerging. This research is motivated not only by envisioned single molecule devices, but also by the conceptual simplicity of such systems that offer convenient platforms for correlating theory and experiment, and by the intrinsic challenge involved in understanding thermodynamic response, both electronic and structural, of molecular species in a transport junction.

This book is devoted to the area of molecular electronics, and to explicating and demonstrating some of its crucial understandings, accomplishments and challenges. This introductory overview chapter addresses the interrelationship among charge transfer, transmission and transport in molecular systems, providing the conceptual framework for molecular electronics. It should be regarded as a sketchy introduction to the field, not a survey. The authors apologize for the many omissions, and the deeply incomplete literature citations, in this chapter. These should be remedied by the wide scope and depth of this book as an entirety.

2 Theoretical Approaches to Conductance

In this section, we give a brief outline of the standard approaches for modeling and understanding transport in MJ. Carbon nanotubes, because of their stiffness and aspect ratio, constitute a special case, and we focus rather on organic molecules.

The simplest interpretation of Scanning Tunneling Microscope images was developed by Tersoff and Hamann [22], and states that the current is proportional to the total density of states at the position of the terminal atom of the

tip and at the Fermi energy. For molecular junctions, this picture is invalid, because the two molecular ends are both in contact with an electrode.

When a molecular structure, acting as a wire, is functionalized to two electrodes, a molecular transport junction is formed. The simplest discussion of transport is then to assume that incoming electrons are scattered both at the interfaces between the metal and the molecule and along the wire itself. Under these conditions, the conductance will depend on the net probability of scattering. An important point first noticed by Landauer [23, 24] is that such scattering does not have to be inelastic – even elastic scattering will prevent electrons making it through the junction. Dissipation of energy will eventually occur, but that can happen in the (macroscopic) leads leading to the molecular junction.

This fundamental realization suggests that the junction resistance in this case arises from its behavior as a scatterer, and its conductance can therefore be calculated simply from scattering theory. This *coherent conductance* is expected to characterize most short molecular wires, particularly those in which transport occurs far from resonance between the metal Fermi energy and the molecular eigenstates,[1] and at low temperature for short wires. Under those conditions, the conductance $g(E, V)$ is given by

$$g(E, V) = \frac{2e^2}{h} \sum_{ij} t_{ij}(E, V) \tag{4}$$

Here the prefactor is the quantum of conductance, and t_{ij} is the probability that a carrier coming from the left lead in transverse mode i will be transmitted to the right lead in transverse mode j.

A more general approach includes not only elastic scattering, but also such issues as interaction between the molecule and the electrodes and the coupling to vibrations and to external fields such as light or thermal gradients. The most common formulation is the Keldysh-Kadanoff-Baym [25–28] one in terms of non-equilibrium Green's functions (NEGF). Reference [29–35] The use of molecular electronic structure theory for the molecule, combined with models for the interface and appropriate treatments (NEGF formulations [29–36], Lippman/Schwinger scattering approaches [37–40]) of the scattering process lead to actual calculations of molecular transport.

In the limit of small applied voltage V, the coherent conductance can be written as

$$g(\Phi) = \frac{e^2}{\pi\hbar} Tr_M\{G^M(\Phi)\Gamma^R(\Phi)G^{M^+}(\Phi)\Gamma^L(\Phi)\} \tag{5}$$

Here the Green's function G^M describes propagation through the molecule, and Γ^R and Γ^L are respectively the spectral densities coupling the molecule to the electrodes on the left and the right. The Tr_M denotes a

[1] Near resonance the possibility for dephasing and relaxation may limit the validity of (4)

trace over the states of the molecule, and G^M is modified from the bare molecule propagator by including the broadening and shifting effects of the molecule/electrode interactions.

The dependence of the conductance on the molecular species arises mostly from the Green's function G in (5). In a very simple single-determinant description, if we use i, j to denote atomic orbitals and μ for molecular orbitals, the matrix elements of G are

$$G_{i,j}(E) = \sum_{\mu} < i|\mu >< \mu|j > /(E - E_\mu - \Sigma_\mu) \tag{6}$$

with E, E_μ and Σ_μ respectively the energy variable, the molecular orbital energy and the self-energy. The self energy is a complex function – its real part describes the shift of the resonance due to interaction with the external partners, while the imaginary part, Γ, characterizes the lifetime of the state. Note that (as is intuitive) the G will maximize when the injection energy E is close to a molecular orbital resonance energy E_μ and when the molecular orbital involved has substantial components from the atomic orbitals i, j on the two ends of the molecule.

A particularly simple junction contains only one homonuclear diatomic (such as H_2), with one basis function on each atom. References [3,41] ignoring electron repulsion and orbital overlap, the two degenerate sites of energy E_0 mix by a tunneling energy t_0. Then the conductance becomes $g(E_F)$ where

$$g(E) = \frac{e^2}{\pi\hbar} \frac{\Gamma|t_0|^2}{|(E - E_0 + (1/2)i\Gamma)^2 - t_0|^2|^2} \tag{7}$$

When injection occurs exactly on resonance ($E_F = E_0 \pm t_0$) and $t_0^2 \gg \Gamma^2$, this behaves as a pure Landauer channel.

$$g = g_0 = 2e^2/h \tag{8}$$

Note that this holds independent of the spectral density Γ, so long as the energy $E - E_0 - t_0$ overlaps with any nonvanishing value of Γ. The elastic current for resonance injection is $g_{0,}$ independent of the (nonvanishing) binding between molecule and electrodes. Experimental reports of near-unit conductance for dihydrogen on platinum at low temperatures [42] may reflect such injection.

One way to produce resonance injection is to move the molecular eigenstate energies by a gating field. Recent work with a molecular transistor injection has indeed observed resonant injection, and $g \cong g_0$, for such molecules as ferrocene [43].

Note that if $\Gamma^2 \ll t_0^2$ but injection is not on resonance (but, say, at midgap), we find [41]

$$g = g_0 \frac{4t_0^2\Gamma^2}{(t_0^2 + \Gamma)^2} \to 0 \tag{9}$$

The conductance then exhibits turnover behavior, vanishing at $t_0 = 0$ (as seen from (7)) because no mixing of the two molecular sites occurs, and at $t_0 \gg \Gamma$, because there is no available spectral density at the orbital resonance energy.

3 The Relationship Between Electron Transfer Rates and Molecular Conduction

We have already noted that electron transfer and molecular conduction are two facets of electron transmission through a molecular environment, and as such should be interrelated. Still this relationship is not a trivial one for several reasons. First, as discussed in Sect. 1 there are fundamental differences between the two processes that arise from different physical boundary conditions. One is driven by nuclear relaxation at the donor and acceptor sites while the other is made possible by absorption of the transmitted electron in the continuum of metal electronic states. Secondly, even though the core process in both situations is electron transmission through a molecular layer or bridge, the fact that in the conduction process one puts a potential across the junction may change the electronic structure of the bridge; at the simplest level this gives rise to a potential gradient on the bridge itself, implying change in local energies. Finally, the two quantities observed, transfer rate in one case and conductance in the other, are different physical observables of different dimensionalities.

Still, the conduction property of a given molecular system and the electron transfer properties of the same system should be closely related at least for low bias potentials and once the different boundary processes have been sorted out. Expression relating the two were recently derived both for the coherent transport regime and for the incoherent hopping regime. Here we limit ourselves to demonstrating the physical issues involved using simple limiting forms. For the coherent transport regime and symmetric electron transfer one finds [3, 44]

$$g \approx \frac{8e^2}{\pi^2 \Gamma_D^{(L)} \Gamma_A^{(R)} \mathcal{F}} k_{D\to A} \tag{10}$$

where g is the zero bias conduction, $k_{D\to A}$ is the donor-to acceptor electron transfer rate, $\mathcal{F}$ is the Franck-Condon weighted density of states thermal environment (see (1)) and $\Gamma_D^{(L)}$ and $\Gamma_A^{(R)}$ represent the inverse escape time of an electron on the donor molecule when next to (say) the left metal electrode, into that electrode, and similarly for the acceptor next to the right metal electrode. Equation (10) is a limiting form obtained when these rates are comparable to, or larger than the inverse energy difference between the metal's Fermi energy and the energy of molecular orbital that is active in the transport process. Another limiting form is obtained for incoherent hopping transfer through a long molecular bridge, provided that energy shifts caused

by the molecule-metal coupling are small relative to k_BT. It reads (again for symmetric electron transfer) [45]

$$g \approx \frac{e^2}{k_BT} k_{D\to A} \tag{11}$$

The simple form of the latter result stems from the fact that for incoherent hopping transmission through a long chain is dominated by dynamics on the chain itself and not at the molecule-lead contacts. Interestingly, and quite accidentally, both (10) and (11) yield at room temperature similar numerical estimates

$$g \sim (e^2/\pi\hbar)(10^{-13} k_{D\to A}(S^{(s^{-1})}) \cong [10^{-17} k_{D\to A}(s^{-1})]\Omega^{-1} \tag{12}$$

when the semiclassical Marcus expression [46] for $\mathcal{F}$ in a symmetric donor-acceptor problem, $\mathcal{F} \approx (\sqrt{4\pi\lambda k_B T})^{-1} \exp(-\lambda/4k_BT)$ is used in (10) together with the value $\lambda = 0.5\,\mathrm{eV}$ for the reorganization energy and the values $\Gamma_D^{(L)} = \Gamma_A^{(R)} \sim 0.5\,\mathrm{eV}$ for the electron escape rates into the electrodes. Actual values of these parameters can of course differ, but these representative values provide an order-of-magnitude criterion for observing conduction in the small voltage-bias regime of molecular conduction junctions. For example, with a current detector sensitive to pico-amperes, $k_{D\to A}$ has to exceed $\sim 10^6\,\mathrm{s}^{-1}$ (for the estimates of $\mathcal{F}$ and Γ given above) before measurable current can be observed at 0.1 V across such a junction. Such estimates should be exercised with caution, both because the above expressions are approximate limiting forms of more complex relationships within the corresponding models and because the models themselves are highly simplified. Still, they may be useful as rough order of magnitude estimates as was indeed found in a recent comparison of electron transfer and conduction through alkane bridges [47].

4 Interaction with Nuclear Degrees of Freedom

Electron transfer processes, as described in Sect. 1 involve electron-phonon coupling in an essential way: this coupling causes the relaxation process that affects electron localization on the donor and acceptor species and thereby drives the transfer process. As discussed in Sect. 2, molecular conduction is driven by a potential difference between two infinite electrodes and phonon induced localization does not play any essential role in affecting this driving. Still, also in molecular conduction, the coupling between electronic and nuclear degrees of freedom is of great interest on several counts. First, it underlines the interplay between coherent transport by carrier tunneling and/or band motion, polaronic conduction and incoherent, thermally assisted hopping transport [3]. Indeed, the importance of the full hopping regime, in which charges are definitely localized on the molecular bridge, has been demonstrated both in the Coulomb blockade limit [48] and in a polaron-type localization situation [49]. Secondly, it is directly relevant to the issue of junction

heating [50–52]. Also, vibronic interactions accompanying electron transport may lead to specific nuclear motions such as rotations [53, 54], lateral hopping of molecules on the surface [55], atomic rearrangements [56] and chemical reactions [57]. Finally, nuclear motions can directly manifest themselves as inelastic signals in the current-voltage spectra. Inelastic electron tunneling spectroscopy (IETS) has been an important tool for identifying molecular species in tunnel junctions for a long time [58]. With the development and advances in scanning tunneling microscopy (STM) and spectroscopy (STS) it has proven invaluable as a tool for identifying and characterizing molecular species within the conduction region [54, 59–62]. Indeed, this is the only direct way to ascertain that a molecular species indeed participates in the conduction process, and at the same time to provide important spectroscopic and structural data on the conducting molecule, in particular information on the strength of the vibronic coupling itself [63].

4.1 Timescale Issues

The relative importance of vibronic (or electron-phonon) interactions in electron transmission processes is an issue of relative timescales. If the transmission event is fast on the timescale of nuclear motion the latter may be taken static, and we only need to average the resulting elastic transmission probability over the relevant ensemble of nuclear configurations. The other extreme limit, where the nuclear motion is fast relative to the electronic process is usually not relevant in our system. Dynamic electron-phonon effects may potentially play a significant role when the electronic and nuclear timescale are similar. In order to make an assessment of this possibility an estimate of the relevant electronic timescale is needed. For resonance electron transfer this timescale is associated with the electronic coupling, e.g. for band motion – by the inverse bandwidth. For off resonance tunneling transmission a useful estimate is provided by the tunneling traversal time, τ_{trav}, essentially a (non-rigorous) estimate of the time available for a tunneling electron to interact with degrees of freedom localized in the barrier region. For example, for a particle of mass m and energy E that tunnel through a rectangular barrier of height U and width D, the traversal time is given by

$$\tau_{\mathrm{trav}} = \sqrt{\frac{m}{2(U-E)}}D \tag{13}$$

while for transmission in the model of Fig. 2b, involving N bridge levels and an energy gap ΔE we obtain [64]

$$\tau_{\mathrm{trav}} = \frac{\hbar N}{\triangle E} \tag{14}$$

It may in fact be shown [64] that both (13) and (14) are limiting cases of a more general expression. For typical molecular parameters, say $D = 1\,\mathrm{nm}$,

$N \cong 2-4$ and $\Delta E = U - E = 1\,\mathrm{V}$ (13) and (14) yield τ_{trav} in the range $0.1 - 1\,\mathrm{fs}$. On this short timescale one may disregard nuclear motion and inelastic effects on electron transmission. We see however that for smaller ΔE inelastic effects may become relevant. In particular this is often the case in resonance tunneling situations. For example, a recent computational study of electron tunneling through water films [65] has revealed the existence of water structures that support resonance tunneling in the energy range of up to 1 eV below the vacuum barrier and with traversal timescales of the order of $\sim$10 fs, similar to the period of the OH stretch vibrations in water.

4.2 Transition from Coherent to Incoherent Motion

In most treatments of electron transmission and conduction through insulating barriers one assumes that the barrier nuclear configuration is static. (This should be distinguished from nuclear relaxation at the donor and acceptor sites in the electron transfer process which is the driving force for this process). The breakdown of this assumption can potentially have far reaching consequences. In the extreme case, energy transfer into nuclear motions from the transmitting electrons may lead to conformation changes and eventually to disintegration of the junction. Indeed, an important factor in designing molecular conductors is their structural stability and understanding processes that can undermine this stability is of utmost importance [66]. A single molecule junction that carries 1 nA of current over a voltage drop of 1 volt passes $\sim 10^{10}$ eV of energy per second, many orders of magnitude more than is needed to atomize its components. This implies the need for understanding heat generation and dissipation in molecular conductors. In the other limit of very weak electron-nuclear interaction, electron transfer and transmission remain essentially the same, still the signature of electron-phonon coupling may be observed as vibrational features in the voltage dependence of the current observed in inelastic tunneling spectroscopy.

In very common intermediate cases, energy does not accumulate excessively in the junction, still interactions with the thermal environments can lead to a fundamental change in the transmission mechanism: Coherent transfer is replaced by incoherent hopping. This can be simply demonstrated [29], for a one dimensional wire problem where, in the linear transport regime, the Landauer formula [29] for the conduction reads

$$g(E) = \frac{e^2}{\pi\hbar}\mathcal{T} \tag{15}$$

where $\mathcal{T}$ is the transmission coefficient and e the electron charge. Consider now a conductor of length L as a series of N macroscopic scatterers. At each scatterer the electron can be transmitted with probability $\mathcal{T}$, or reflected with probability $\mathcal{P} = 1 - \mathcal{T}$. Let the the total transmission through N such objects be $\mathcal{T}_N$, so that $\mathcal{T} = \mathcal{T}_1$. *Provided that the phase of the wavefunction is destroyed after each transmission-reflection event*, so that we can add

probabilities, the transmission through an N scatterers system is obtained by considering a connection in series of an $N-1$ scatterer system with an additional scatterer, and summing over all multiple scattering paths

$$\mathcal{T}_N = \mathcal{T}_{N-1}(1 + \mathcal{R}\mathcal{R}_{N-1} + (\mathcal{R}\mathcal{R}_{N-1})^2 + \ldots)\mathcal{T} = \frac{\mathcal{T}\mathcal{T}_{N-1}}{1 - \mathcal{R}\mathcal{R}_{N-1}} \tag{16}$$

with $\mathcal{R} = 1 - \mathcal{T}$ and $\mathcal{R}_N = 1 - \mathcal{T}_N$. This implies

$$\frac{1 - \mathcal{T}_N}{\mathcal{T}_N} = \frac{1 - \mathcal{T}_{N-1}}{\mathcal{T}_{N-1}} + \frac{1 - \mathcal{T}}{\mathcal{T}} = N\frac{1 - \mathcal{T}}{\mathcal{T}} \tag{17}$$

so that

$$\mathcal{T}_N = \frac{\mathcal{T}}{N(1 - \mathcal{T}) + \mathcal{T}} = \frac{L_0}{L + L_0} \tag{18}$$

where $L_0 = \mathcal{T}/V(1 - \mathcal{T}$ and $v = N/L$ is the scatterer density. Using this transmission coefficient in (15) yields

$$g(E) = \frac{e^2}{\pi\hbar}\frac{L_0}{L + L_0} \tag{19}$$

that gives the inverse length dependence characteristic of Ohm's law as $L \to \infty$.

More detailed treatments can handle situations where dephasing is not complete at each scatterer. Büttiker [67] has introduced phase destruction processes by conceptually attaching an electron reservoir onto the constriction under the condition that, while charge carriers are exchanged between the current-carrying system and the reservoir, no net averaged current is flowing into this reservoir. Such a contact, essentially a voltage probe, acts as a phase breaking scatterer, and the dephasing efficiency is controlled by adjusting the coupling strength between this device and the system. A very different approach to dephasing was considered by Bixon and Jortner [68, 69] who pointed out that the irregular nature of Franck Condon overlaps between intramolecular vibrational states associated with different electronic centers can lead to phase erosion in resonant electron transfer. Yet another approach uses the machinery of non-equilibrium statistical mechanics, starting from a Hamiltonian that includes the junction and its thermal environment and deriving reduced equations of motion for the electron dynamics. This leads to a dynamical description that includes the effect of dephasing and energy relaxation that are characterized by properties of the thermal bath and the system-bath coupling.

Figures 3–8 show some theoretical results based on the latter approach and recent experimental results that show the effect of dephasing and activation [70, 72]. While the transition from tunneling to activation dominated rate processes has been known in other rate phenomena, the manifestation of this transition in the length dependence of tunneling conduction or electron transfer rate is a relatively recent development. Table 2 [73] summarizes these results for the Markovian limit of the thermal relaxation process.

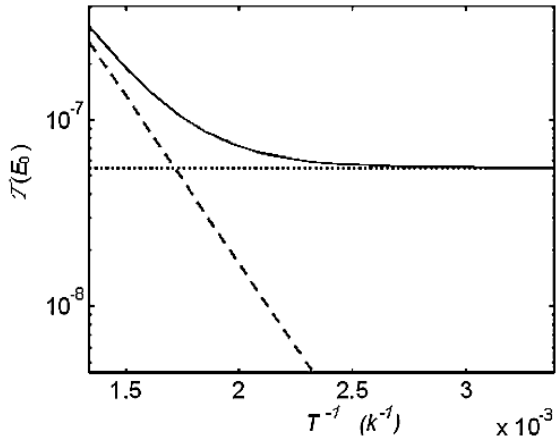

Fig. 3. The integrated elastic (*dotted line*) and activated (*dashed line*) components of the transmission (zero bias conduction), and the total transmission probability (*full line*) displayed as function of inverse temperature (from [50])

Table 2. Bridge length dependence of the transmission rate [73]

Physical Process	Bride Lenghth (N) Dependence	
Super exchange ($small\, N$, $large\, \Delta E_B/V_B$, $large\, \Delta E_B/k_B\mathsf{T}$)	$e^{\beta N}$	$-\beta' = 2\ln(V_B/\Delta E_B)$
Steady state hopping ($large\, N$, $small\, \Delta E_B/V_B$, $small\, \Delta E_B/k_B\mathsf{T}$)	N^{-1}	
Non-directional hopping ($large\, N$, $small\, \Delta E_B/V_B$, $small\, \Delta E_B/k_B\mathsf{T}$)	N^{-2}	
Intermediate range intermediate N, small $\Delta E_B/V_B$	$(k_{up}^{-1} + k_{\rm diff}^{-1}N)^{-1}$	$k_{up} \sim (V_B^2 k/\Delta E^2)e^{-\Delta E_B/k_BT}$ $k_{\rm diff} \sim (4V_B^2/k)e^{-\Delta E_B/k_BT}$
Steady state hopping + competing loss at every bridge site	$-e^{\alpha N}$	$\alpha = \sqrt{\Gamma_B(\Gamma_B + k}/2V_B$

Notation: N-site bridge, with intersite electronic tunneling matrix element V_B, injection energy barrier E_B, temperature T, friction coefficient (inverse dephasing time) κ.

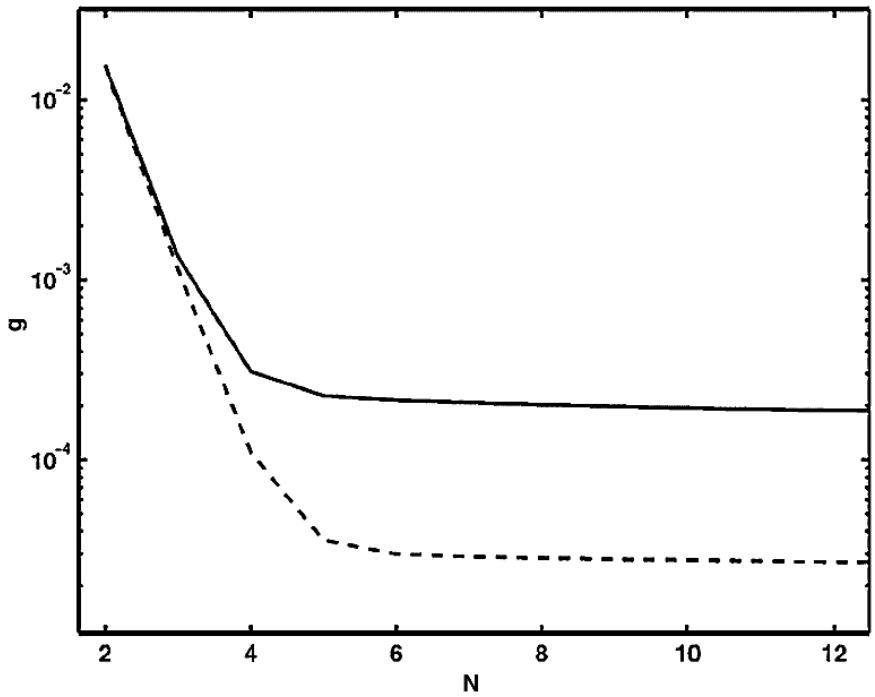

Fig. 4. Bridge length dependence of molecular conduction (or electron transfer rate), showing the transition from exponential decrease with chain length for short chains to a weak $(k_1 + k_2 N)^{-1}$ dependence at long length. The parameters used in this calculation are $\Delta E = E_B - E_F = 0.2\,\text{eV}, V = 0.05\,\text{eV}.\Gamma_L = \Gamma_R = 0.1\,\text{eV}$ and the rate of thermal relaxation 0.01 eV, and the results shown are obtained using temperatures of 300 K (*lower curve*) and 500 K (From [50])

4.3 Heating and Heat Conduction

As already noted, a molecule that carries 1nA of electronic current across a potential bias of 1 V is passing $\sim 10^{10}$ eV of energy per second. A tiny fraction of this energy, if it remains on the molecule for more than a few ps, will cause molecular ionization or dissociation and disintegration of the junction. With the objective of achieving a stable conducting operation (as opposed to, say, inducing a chemical reaction by passing a current) two questions are in order. First, what is the rate of electronic energy dissipation (heat generation, i.e. increased nuclear kinetic energy) on the molecular bridge and, second, how fast is the heat transfer out of the molecule, into the surrounding environment. The most challenging situation is that where heat can flow from the molecule only onto the electrodes with which it is in contact.

For a molecule that carries a current I under a potential bias Φ in a steady state operation, the answer [74] to the first question is $\kappa I \Phi$, where

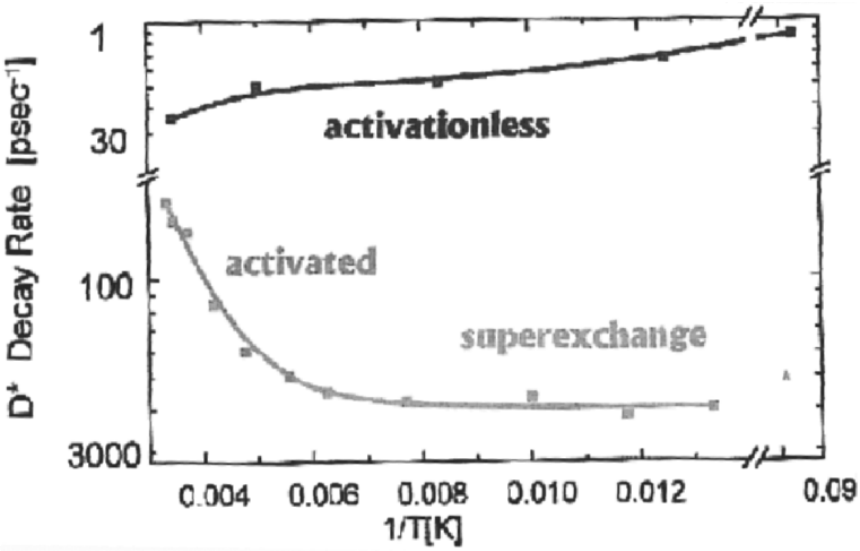

Fig. 5. Temperature dependence of the electron transfer rate in the photoreaction center (G. Hartwich, G. Bieser, T. L. Angenbachen, P. Müller, M. Richter, A. Ogrodnik, H. Scheer and M.E. Michel-Beyerle, Biophys. J. 71, A8 (1997); see also M. Bixon and J. Jortner, [11]). The activationless behavior (upper curve) corresponds to the wild-type reaction center while crossing from super-exchenge at low temperature to activated behavior at higher T is exhibited in a chemically engineered reaction center in which the bacteriochlorophyl is replaced by vinyl bacteriochlorophyl

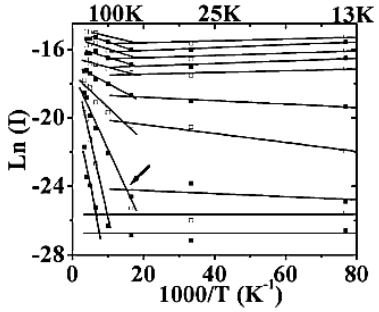

Fig. 6. Temperature dependence of the current through 1-nitro-2,5-di (phenylethynyl- 4' -mercapto) benzene molecules between gold electrodes, showing transition from non-activated to activated behavior with a bias-dependent activation energy (After [70])

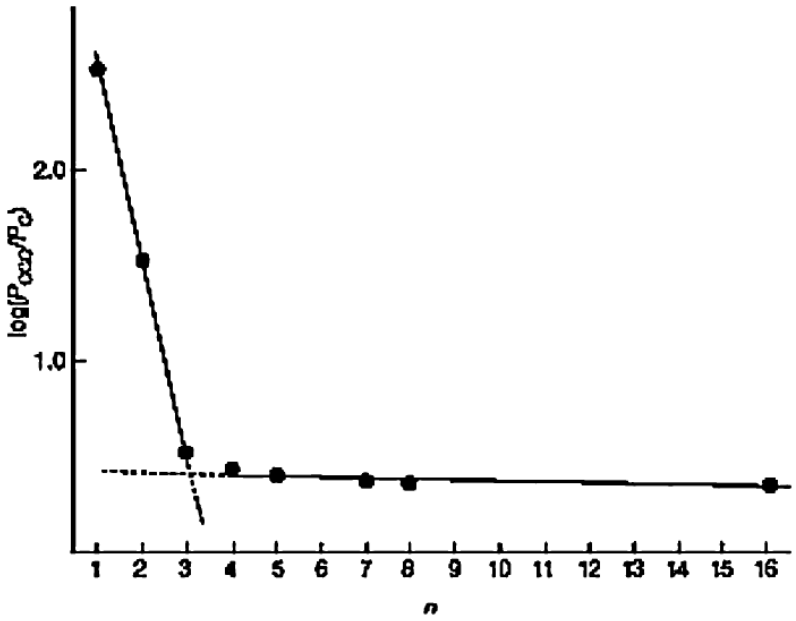

Fig. 7. Measured length dependence of electron transfer yields in DNA (from [71])

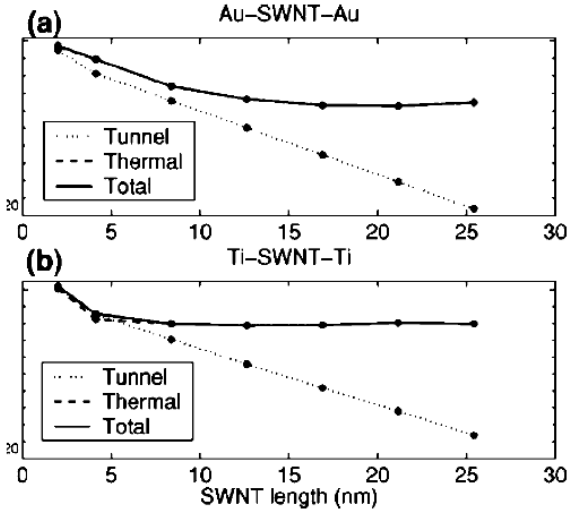

Fig. 8. Room temperature calculated conductance of a single-walled nanotube between gold electrodes, as a function of nanotube length. (from [35])

$0 \geq \kappa \geq 1$. A calculation based on a tight-binding model [74] with electron-phonon coupling estimated from molecular reorganization energies yields κ of order 0.1. Thus the heat conduction problem in molecular junctions becomes crucial. As a zero-order approximation one may try to represent the molecular wire as a cylinder characterized by the classical heat conduction coefficient of saturated organic materials. This yields the results [74] of Fig. 9 that may lead us to conclude that the temperature rise expected under reasonable operating conditions is not significant. It appears though that using classical heat conduction for such estimates fails for two reasons. First, the size of molecular conduction bridges is often small enough to make phonon motion essentially ballistic and classical heat conduction concepts largely invalid. This actually enhances heat transfer out of the molecule relative to what is expected in macroscopic, diffusive, conduction. On the other hand, small molecular systems are restricted environments, limited in the number and spectrum of available phonon modes. This reduces the efficiency of heat dissipation out of the molecule and the net outcome [51], as we know from experiment, is that junction stability may be compromised by passing current through its molecular component.

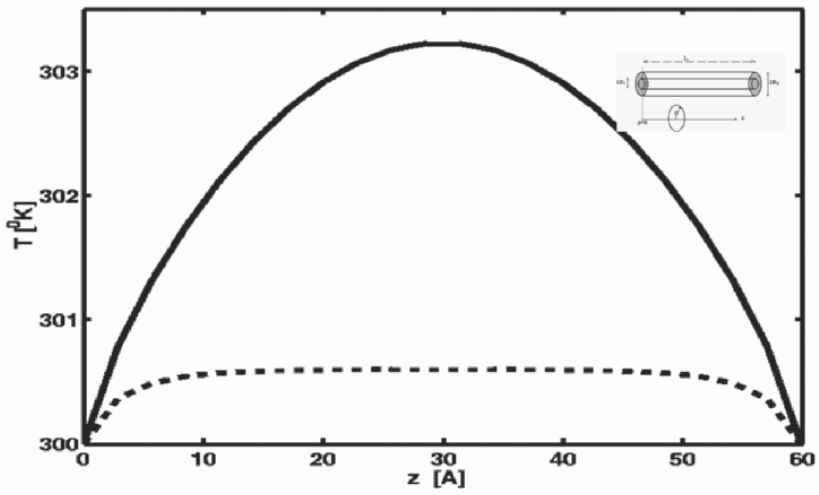

Fig. 9. A model estimate of the temperature rise of a current carrying molecular junction (model as a cylinder (see inset) connecting the electrodes). Heat is assumed to be deposited at the center of the cylinder at a rate of 10^{10} eV/s (an estimate from a theory based on the Redfield formalism for a current of 10 nA at voltage 1 eV) and the classical heat equation. With heat conduction $\sigma_h = 3.5 \cdot 10^{-4}$ cal/(s · cm · K) typical of organic solids is used to estimate the cooling. (from [73]). The length of the cylinder is 60 Å. The *upper curve* is obtained from a calculation that assumes that heat flows out of the molecule only at the contacts with the leads. The *lower curve* is from a calculation that assumes cooling through th entire molecular surface

4.4 Inelastic Electron Tunneling Spectroscopy (IETS)

Inelastic tunneling spectroscopy, an increasingly important tool for studies of molecular conduction junctions, provides the possibility to view directly the consequence of electron-phonon interaction in the tunneling current. Experimentally one looks for vibrational signatures in the current/voltage response of the junction. An important technical difference between IETS and electronic optical spectroscopy is that in the latter case the energy of the observable (light) is easily resolved, while a current is an integral over energy (see (3)) that needs to be differentiated to get energy resolved information.

Vibrational signatures in the current-voltage relationships of molecular junctions can stem from two origins (see Fig. 10a). At the threshold where the potential bias between the left and right electrodes exceeds $\hbar\omega_0$, where ω_0 is the frequency of a nuclear vibrational mode on the bridge, the tunneling electron can exchange energy with this mode and the additional inelastic signal is observed as a conduction step, i.e. a peak in the second derivative $d^2I/d\Phi^2$ of the current with respect to the voltage. If the potential bias is such that an electronic level of the bridge just enters the window between the Fermi-energy of the two electrodes, resonance tunneling takes place and the corresponding peak in the conductance $dI/d\Phi$ may be accompanied by satellite vibrational peaks similar to those observed in resonance Raman scattering. An example of the resulting spectroscopy is shown in Fig. 12 of Chap. 30. References [61, 75] discuss recent observations of vibrational structures dressing resonance tunneling currents.

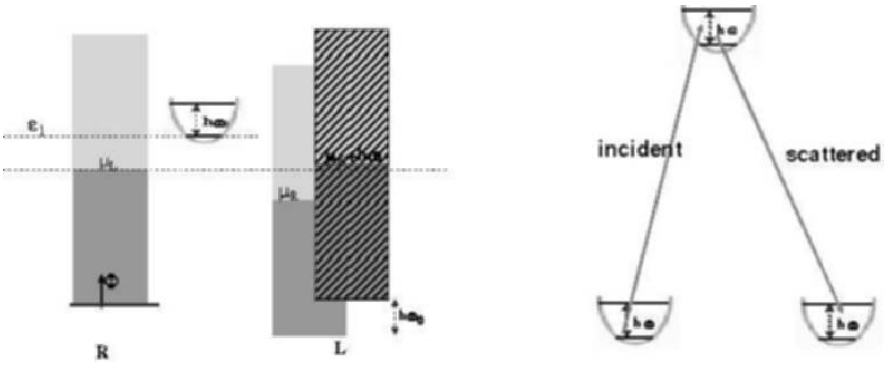

Fig. 10. A schematic view of the level structure for inelastic electron tunneling (*left*) and for Raman scattering (*right*). The shaded areas in left figure denote the continuous manifolds of states of the two leads where the lines separating the occupied and unoccupied states are the corresponding Fermi energies. For the right lead two manifolds are shown: one where the corresponding molecular state is the ground vibrational state of the molecule, and the other (*diagonally shaded*) where the molecule is in the first excited vibrational state. The horizontal dotted lines at heights μ_L and ε_1 are added to guide the eye

At the threshold $|e\Phi| = \hbar\omega_0$ of the inelastic tunneling channel both the elastic and the inelastic fluxes change, with the latter obviously increasing from its zero value below threshold. In contrast, as first noted by Persson and Baratoff [76], depending on the energetic parameters of the system, the correction to the elastic current may be negative. Furthermore, this negative change in the elastic tunneling component may outweigh the positive contribution of the inelastic current, leading to a negative peak in the second derivative of the current/voltage relationship. Such negative features have indeed been observed in recent single-molecule IETS studies [60, 71]. It should be noted that not only the sign but also the shape of these peaks depend on the energetic parameters of the system [77], and recent results [62] (see also Chap. 30) that show relatively strong derivative-like features in the low temperature IETS spectrum of C8 alkane thiols may be another manifestation of the same effect. The origin of this rich range of behaviors is the interference between different orders (in the electron-phonon coupling M) of the elastic contribution to the tunneling current, as explained by Fig. 11. This figure refers to a simple model [77] with a single bridge electronic state (1) and a single phonon mode, described by the Hamiltonian

$$\hat{H}_0 = \varepsilon_1 \hat{c}_1^\dagger \hat{c}_1 + \sum_{k\epsilon L,R} \varepsilon_k \hat{d}_k^\dagger \hat{d}_k + \omega_0 \hat{a}^\dagger \hat{a} + \sum_{k\epsilon L,R} (V_{k1} \hat{d}_k^\dagger \hat{c}_1 + h.c.) + M(\hat{a}^\dagger + \hat{a}) \hat{c}_1^\dagger \hat{c}_1 \tag{20}$$

where $\hat{c}_1^\dagger$ and $\hat{c}_1$ are creation and annihilation operators for electrons on the bridging level of energy $\varepsilon_1, \{k\} = \{l\}, \{r\}$ are sets of electronic states representing the left (L) and the right (R) electrodes with the corresponding

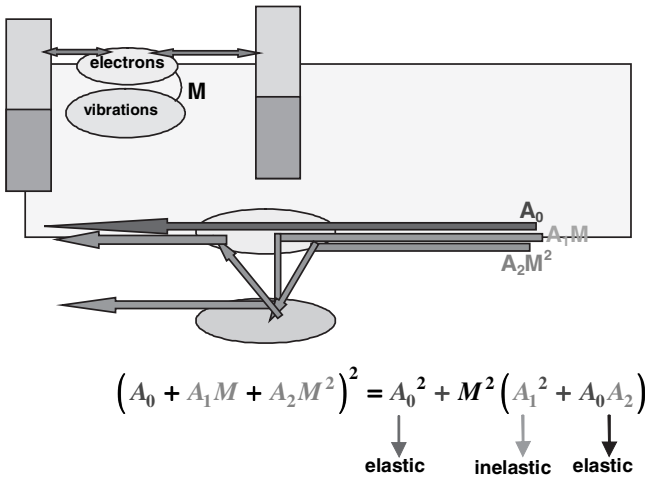

Fig. 11. A scheme used to explain the low order elastic and inelastic components of the IETS signal. See text for details

creation and annihilation operators $\hat{d}_k^\dagger$ and $\hat{d}_k$ and $\hat{a}_k^\dagger$ and $\hat{a}$ are creation and annihilation operator for the phonon mode of frequency ω_0. The tunneling amplitude may be written, to second order in the electron-phonon coupling M as $A = A_0 + A_1 M + A_2 M^2$ where A_0 is the amplitude of a zero order process that involves no phonons, A_1 is a 1-phonon inelastic tunneling amplitude and A_2 is a 2-phonon elastic amplitude that describes a second order process where one phonon was created then destroyed. Clearly, the intensity A^2 contains in second order contributions of inelastic process, and interfering elastic processes as seen in Fig. 11.

5 Remarks and Generalities

Since junction transport is in some senses an extension of non-adiabatic molecular electron transfer, conductances and rate constants are closely related (Sect. 3), and both undergo characteristic changes between coherent and incoherent motion mechanisms (Sect. 4). Because of these similarities, there are a number of common issues that will arise in the measurement of either conductance or electron transfer rates. These are discussed in Sect. 5.1 of this chapter. There are, however, some special aspects of junction transport, that arise from the nature of the states and the dynamical processes involved. These aspects are discussed in Sect. 5.2.

5.1 Electron Transfer and Conductance: Common Issues

Electronic States

Because charge transfer or transport is the defining process, both ET and JC (electron transfer and junction conductance) deal with initial and final electronic states. In junctions, the electronic states in question lie within the continuum of the leads. For ET, both the initial and final states are isolated molecule electronic eigenstates. Nevertheless, the transport coefficients (k_{ET} and g) will vary with varying initial or final electronic state. While this has been extensively investigated in the ET field [1, 78, 79] (in particular using photoelectrochemistry), it is also expected to be present in junctions: indeed, photoexcited junction transport has been discussed in the theoretical literature [80], and some initial experimental aspects are beginning to appear [81].

Electron Correlation

The electron correlation problem enters into both processes. This term refers to the fact that interelectron repulsion both makes the electronic structure of molecules or solids a problem that is impossible to solve exactly, and substantively modifies energy levels. In most treatments of ET or MJ, a major simplification is made in that only the single electron terms of a model Hamiltonian

are used: these models are sometimes called tight binding [82], or extended Huckel or one electron. Electron repulsions cause major changes in the properties of individual molecules (for example, they change the optical spectra qualitatively, they are responsible for bond formation and taking them into account is the dominant reason why electronic structure calculations in 2004 are better than they were in 1946).

Calculations employing electronic correlation, often using density functional theory, are now becoming standard both in transport [29–41, 83] and in transfer, but nevertheless major problems still inhere in dealing correctly with the effects of correlation. A specific instance involving junction behavior will be discussed in Sect. 5.2.

Spin Effects

Because of the Exclusion Principle, interactions between same spin and opposite spin electrons are different. In ET, these spin effects are strongly marked in situations involving particular open shell transition metal ions, notably cobalt. In junction transport, there have been a number of theoretical analyses of possible spin effects [84]: one idea is that the spins are polarized in the metallic electrode, and the amplitude for scattering through the junction for same spin and differing spin electrons will differ. The opposite limit involves non-singlet states on the molecule itself. No experimental observations of such phenomena are yet reported. There is also an interesting issue of spin quantization axis, since the two electrodes and the molecule might have quite differing spin axes.

Geometry

It has already been stressed that to obtain useful structure/function relationships, one needs to know structure. Electronic structure calculation for individual molecules can give bond lengths and bond angles, for stable organics, that are essentially as exact as experiment. For ET reactions, then, the geometry problem is to some extent computationally solved. In stark contrast, with the possible exception of nanotubes, nearly nothing is known experimentally about the actual geometry of molecules in transport junctions: this is a non-equilibrium situation, and non-equilibrium methods are required to calculate such geometries. There have been some attempts in this direction [85], but since experimental determination of the geometries is so very difficult, it is not known how accurate such calculations are.

5.2 Junction Conductance

Because ET is one of the most important reactions in chemistry, the issues discussed in Sect. 5.1 of this chapter have been investigated there both theoretically and experimentally. Since studies of JC are essentially only a decade

old, and since the metrical problems are so serious, much of this territory has been unexplored. But other effects can dominate in junction transport, and these differentiate the ET and JC situations.

Geometric Behavior

Modifications in structure lead to modifications in molecular properties; such structure/function relationships are at the heart of modern chemistry. In JC, as already stated several times, the geometries are effectively unknown, and indeed there does not seem any direct scattering method that can be used experimentally to find accurately the geometry of a molecule made of first row atoms in the presence of a large number of metal or semiconductor atoms constituting the electrode. Indirect structural analysis, using vibrational spectroscopy and scanning probe information, is becoming available [62,86]. Until such geometric information permits comparison with computations both of the structure and of transport with different structures, this will comprise a very serious difficulty for accurate comparison between modeling and experiments. Beautiful experiments have demonstrated that electronic currents in junctions can actually break chemical bonds, excite vibrations, and otherwise alter the structural chemistry of the molecules of these junctions [53,54,57,59–61,74]. Understanding that variation remains a major task.

Voltage Profiles

The issue of voltage profiles, effectively the electrochemical potential across a junction in a non-equilibrium state, can be crucial in determining behaviors. This has been studied beginning with a clarification by Datta and his collaborators of the importance of the voltage drop structure [87]. Figure 12 shows some calculations of the local electrostatic field across a model wire system in the Huckel drescription [88]: notice the change in shape from the simple ramp (which is correct in the absence of any charge within the junctions) to a highly screened interaction in which most of the field drops at the electrode/molecule interface. The extent to which a voltage drop occurs at any given spot can only be determined by a self consistent calculation that takes into account carrier-carrier interactions, because it is necessary to solve simultaneously the Poisson equation for the electrostatics and the Schrödinger equation for the wave function. The smooth curves in Fig. 12 come from solving these equations simultaneously for a simple junction model of a wire. In more extensive calculations on the molecules, there have been attempts to describe the electrostatics. Figure 13 shows the calculated electrostatics for a junction consisting of an organic between gold electrodes [89]. There are substantial changes in the potential due to the presence of electrical charge

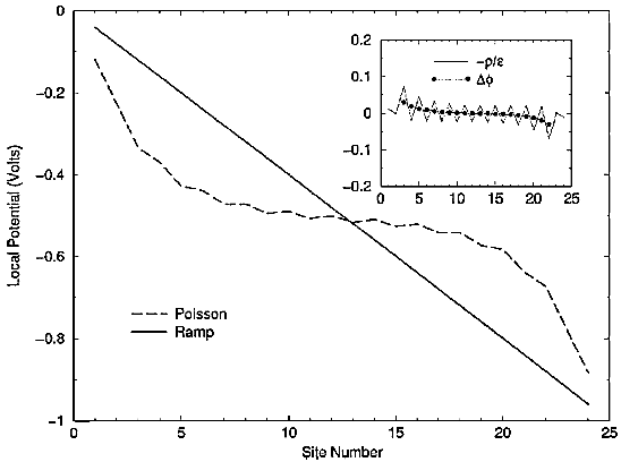

Fig. 12. The effective electrostatic potential acting across a Huckel-level molecular wire contacting two metallic electrodes. The potential indicated as Poisson is a self-consistent solution to the Poisson and Schrodinger equations, while the ramp is simply the applied electrostatic potential. The inset shows the second derivative of the potential(*solid*) and the density divided by the local dielectric constant (*broken*). After [88]

distributions, as is to be expected. Note also that although some of the potential drops at the interfacial regime, substantial amounts do drop across the molecular structure itself.

Understanding the generalities of the voltage profile is crucial, because different voltage profiles will give different solutions to the Schrödinger equation, and therefore different transport predictions. Self consistent field calculations using density functional methods are becoming the standard here [89–91], and can be used to approximate the charge distributions, and therefore the voltage profiles, once self consistency is obtained.

Heuristically, if current is to be continuous throughout the junction, and if Ohm's law were to be obeyed, then the local drop in potential should be proportional to the local resistance. It follows from this argument that if the mixing at the interface is weak, much of the voltage will drop at the interface, and this seems to be borne out by calculations.

Creative work by the McEuen and his collaborators in carbon nanotubes has measured [92] the electrostatic potential, essentially by scanning a voltage probe across the molecule at a functional junction. They observe specific drops along the tube, which are attributed to defects. The actual drop at the interface cannot be measured, because the interface geometry is simply too tight. Measurements of energy dissipation suggest major drops in the field at the interface, as is to be expected. While such measurements would be very

helpful for small molecule circuits, the short length (∼1 nm) makes them very difficult.

The simplest way to think about such effects is to consider that molecules act like polarizable capacitors in junctions, and that the molecular charge distribution polarizes itself to offset the applied field. In this sense, the interface looks slightly like an electrochemical double layer.

The superexchange mechanisms, as detailed above, suggest that whichever effectively coupled frontier level is closer in energy to the injection energy in the junction case, or closer in energy to the donor in the ET case, should dominate the rate constant. Analysis is more difficult with the junctions, only because so many levels of the "extended molecules" enter. For example, very recent calculations by the Bredas Group [93] and by Basch and collaborators [93] have demonstrated that the effective levels of the extended molecule are not the HOMO and the LUMO, because of the importance of metal-induced gap states [94]. Important, strongly coupled levels can be found by population analysis, and for the simple benzenedithiol case there are of the order of a dozen intervening in the extended molecule [93].

Classically, one expects that the presence of a charge distribution near a metal will result in polarization of the metal, and that this polarization can be well described in terms of an image potential picture. Computationally, using electronic structure methods to calculate this image is difficult [96], essentially because of the interelectronic repulsions in the metal. It is not clear how well any of the "extended molecule" schemes currently in vogue for calculating junction transport deal with the very important image problem, nor is it really clear how to include the image heuristically (double counting of image effects must be avoided). Very recent work by the Purdue group [95] has used a self consistent solution to the Poisson equation with an image correction, within a semiempirical CNDO model Hamiltonian. They calculate both the effective voltage profile and the I/V characteristics. The results show rectification behavior, agreeing very well with break junction transport measurements [99].

Electron Correlation

An important set of phenomena directly related to electron correlation effects is characteristic of mesoscopic physics, and is beginning to be observed in molecular junctions. One of these is the so called Kondo effect [48], in which there is actually a maximum in the conductance at zero voltage, if there is an odd spin on the molecular bridge. Effectively, this comes because of exchange interactions creating a very small peak in the density of the states at the metallic Fermi level. The strength of these interactions is characteristically weak, and (Fig. 14) the Kondo maximum disappears at higher temperature. The possible engineering of molecules to give a larger Kondo-like peak constitutes a significant challenge both for experiment and for theory.

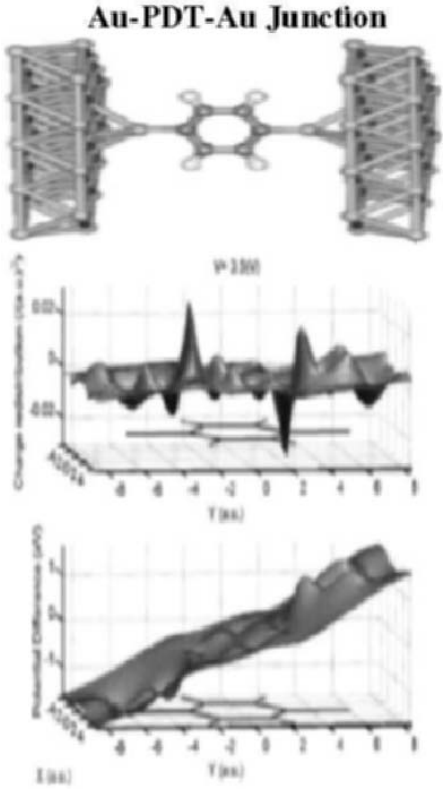

Fig. 13. The difference in electrostatic potentials between the molecule plus electrode and the junction under voltage. The center frame shows the calculated charge transfer, using a very reduced basis set. After [89]

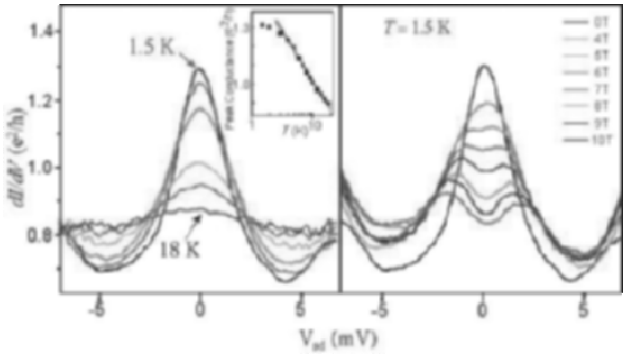

Fig. 14. The observed Kondo-type resonance in the transport through a dithiolated odd-spin Co complex between gold electrodes. Note the disappearance of the resonance peak with increase of temperature. After [48]

When the interfacial mixing (the spectral densities) of the two electrodes become weak, the molecule can act as, effectively, a perfect extended quantum dot structure. Figure 15 shows the observation of the so called "coulomb blockade" structure for a bridge consisting of a gold dot linked to the electrode by duplex DNA strands. The characteristic blockade steps correspond to the charging of the dot, and are seen because of weak effective spectral densities of the two electrodes. Such coulomb blockade structures have been observed in many other molecules [48], and in particular an actual coulombic staircase structure has been reported for a long oligomer of paraphenylenevinylene [49], where a combination of multielectron effects and vibronic interactions is responsible for the multiple charging of the bridge.

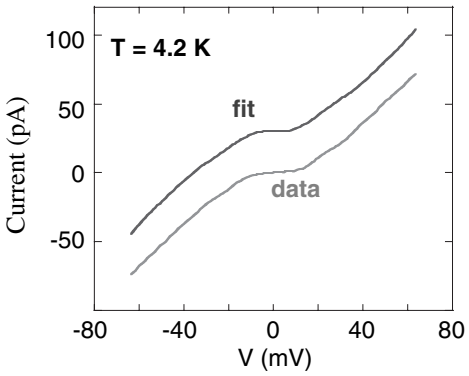

Fig. 15. The coulomb blockade spectrum of a DNA-functionalized Au dot between Au electrodes. The fit is to the standard two-resistor, two capacitor equivalent circuit. After S-W. Chung et al., submitted to Small

Computational Approaches

While use of simple models such as the Newns/Anderson form for the electrode spectral density (based on a one-dimensional tight binding metal) [97] or a Huckel [95] or tight-binding form [82] for the molecular Hamiltonian are extremely useful for understanding general behaviors, there is extensive current activity in actual electronic structure calculations of junction conductance. One approach uses a jellium model for the electrodes and a scattering picture in terms of the Lippman-Schwinger equation for the molecule. This has been extensively applied [37–40], and has a particularly attractive aspect in using a generalized Ehrenfest approach to allow actual geometry optimization under current-flow conditions [85].

More commonly, the junction is broken into two parts, an "extended molecule" consisting of the actual molecule and a few electrode atoms at each end, and the reminder of the electrodes. The latter are represented in terms of their

surface Green's functions, and act as source and drain. The extended molecule is treated using a chosen electronic structure model [29–36]. The choice of method and the basis set determines the quality of the calculation, and self-consistent solution of transport and electronic structure allows prediction of the voltage-dependent conductance. Usually, some form of static Density Functional Theory (DFT) is used for the electronic structure problem.

There are substantive difficulties here, including the fact that static DFT does a very poor job of representing electron injection or ionization processes (essentially the content of the G in (5)), and the balance problem between the basis sets on the molecule and the metal atoms [83,98]. Several contributions both in this book and elsewhere [98] describe alternate, sometimes more sophisticated electronic structure approaches. Since ab-initio methods using correlation corrections of the coupled cluster or Moller-Plesset type do a quite good job in describing ionization and electron capture, their use for conductance seems promising. Basis set issues might be simplified by going to plane-wave formulations.

Reliability, Reproducibility, Experimental Conditions and Switching

Because junction transport is such a new measurement, the community continues to seek the most effective ways to make voltage spectroscopic measurements of transport. Several of the important schemes for doing so will be outlined in the following chapters of this book. In general, however, the measurements break down into two major categories. First, there are break junction measurements [42,99,100], fabrication schemes [101], particular limits of crossed-wire, STM and nanodot collection measurements [102–104], in which one is presumably measuring a small number (ideally 1) of molecules. Second are measurements on adlayers, in which many thousands of molecules can contribute to the transport [105,106]. There is no necessary reason why these two sorts of measurement should give the same current/voltage signatures, even if the molecules are identical, and the electrodes are identical [107]. There are several reasons why such disparities might exist:

First, the spectral densities (effective inverse contact resistance) could vary between adlayers and single molecules. Indeed, calculations indicate [108] (and measurements of adlayer stability and motion also suggest [109] that there are several stable sites for the most common geometries, such as thiol/gold or siloxy linkages [110]. These different geometries are also calculated to have different spectral densities, and therefore different conductance signatures [108]. This is almost certainly the reason for the often-observed striking switching in time dependent measurements of transport. Figure 16 shows an important contribution from the Weiss laboratory [104], with switching on and switching off of transport through a conjugated molecule in a mixed adlayer film. Figure 17 shows the histograms observed by Tao's group [111], found by an electrochemical break-junction scheme. This

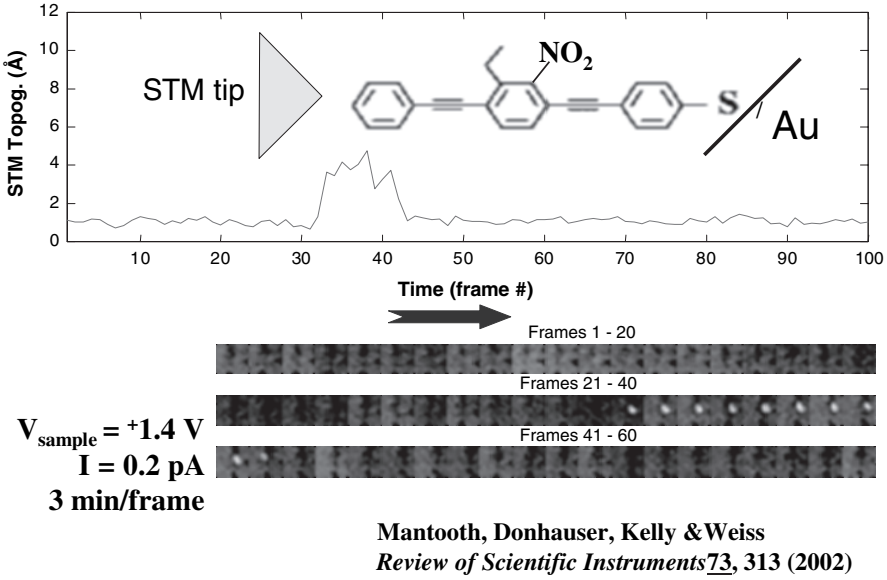

Fig. 16. The observed fluctuations in the transport current to an STM tip probing a pi-type thiol in an adsorbed self-assembled monolayer. Note the strong fluctuations in the current with time. After [104]

is an important measurement, demonstrating clearly the differing conductance values expected for differing geometries. Reed's Group [112] has reported significant conductance fluctuations in disordered SAM structures, but far better reproducibility for ordered ones. For stable organics bound to Si electrodes, fluctuations are very small [100, 101]. The simplest and most persuasive argument for observed conductance switching is indeed geometric change of the environment, just as it is for single molecule spectroscopy and spectral diffusion. Given these different possible geometries and resulting different conductances, it is not surprising that any individual measurement of transport could differ from another.

Second, the presence of self-assembled monolayers on surfaces changes both the work function and the Fermi energy of the metal [113]. Since the Fermi energy enters into the voltage profile, and into the injection gap, it is clear that a given molecule may have a different conductance signature in the presence of an adlayer film than it would on a bare metal, independent of any geometric change.

Given these realizations, it is clear that extensive comparative measurements will have to be made before actual current/voltage/Fermi level behavior is clarified.

Probably the simplest multiple-molecule situation involves alkane thiol adlayers: these are very regular and relatively stable. Moreover, the very

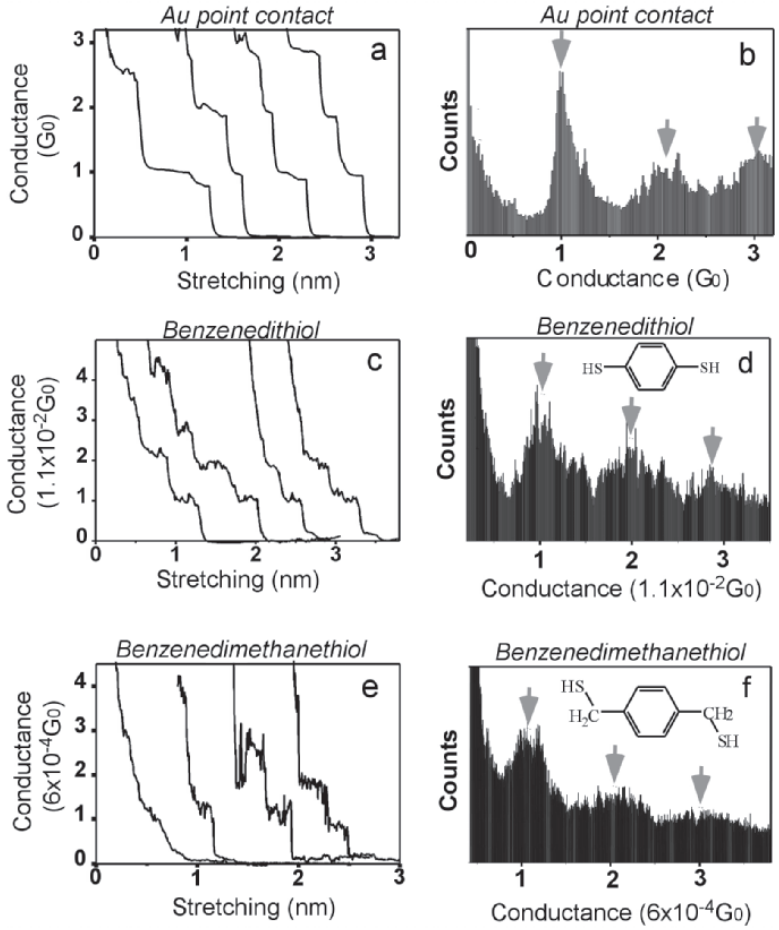

Fig. 17. Histograms for molecular junction conductance observed in an electrochemical environment. The histograms are based on multiple samples, obtained in an electrochemical break-junction measurement. Note the breadth of the observed conductance, the near-quantized transport in the metal wires, and the higher transport in the benzene dithiol than in the xylene dithiol. After [111]

large gap expected due to the saturated electronic structure of the alkane suggests (for example using the Buttiker–Landauer time scale) that here transport will occur by simple quantum mechanical barrier tunneling, expected to follow roughly the Simmons equation [114] and to exhibit no temperature dependence. Precisely these characteristics have been observed in several laboratories [105, 115] – the transport is indeed temperature independent, and indeed decays exponentially with length as would be expected for alkanes. Calculations from several laboratories on such systems agree very well with the experiment for the slope of the exponential decay [116,117]. Nevertheless,

interface effects, electrode instabilities and fabrication problems continue to haunt transport measurements [118].

While stochastic switching arising from thermal or voltage-driven geometry changes can complicate the interpretation of conductance, using controlled molecular geometric changes to modify transport may be a very significant aspect of molecular electronics. Several theoretical papers address the idea of using a stereochemical change [119–121], driven by the applied field, to switch a molecular geometry and therefore to use the molecule as a dynamic circuit element, producing a switch or rectifier. It was pointed out by Datta and collaborators that the use of a standard FET geometry is difficult for molecular species, because the short molecular lengths (of order 1nm) would require a very thin oxide layer (less than the molecular length) for effective switching [122]. Using a stereochemical switch in a two-electrode (source/drain) rather than the three-electrode (source/gate/drain) structure of the traditional FET would constitute a particularly neat form of true molecular electronics (Fig. 18) [119–122].

Other switching phenomena, and indeed a very different set of conductance behaviors, occur when semiconducting electrodes replace metallic ones [101, 102]. It has been demonstrated [100] that reproducible negative differential conductance spectra can occur in transport through a chemisorbed

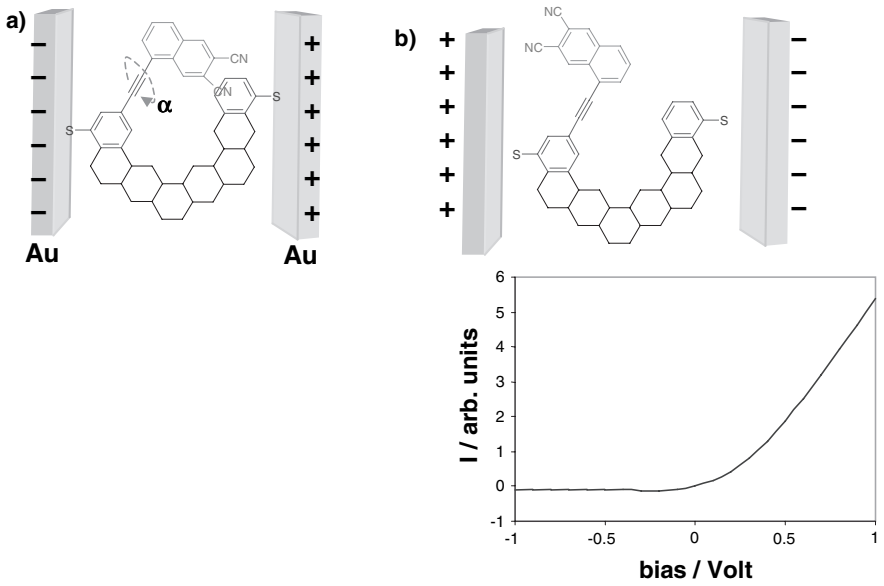

Fig. 18. A proposed molecular junction switch based on rotation about an intramolecular triple bond. Upon changing bias direction, the isomerization substantially changes pi overlap, changing the ambient predicted conductance by more than a factor of 100. After [121]

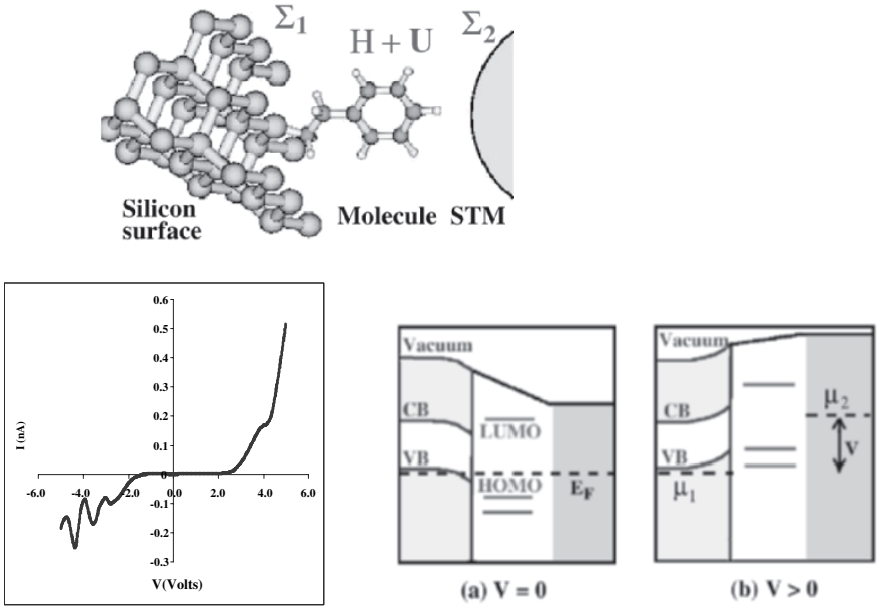

Fig. 19. Observed negative differential conductance in a Si-based molecular junction. The structure is made by adding a free-radical molecule, called tempo, to a single surface dangling bond on a heavily-doped Si single crystal. The conductance fluctuations arise from the bandgaps in Si. After [100]

molecular species on a Si electrode (Fig. 19). Such switching behavior in a stabile geometry, which might be very valuable in actual computational circuitry, can be understood in terms of the bandgaps in the semiconductor electrode [122].

For most interesting molecules, convergence between experiment and theory has been more difficult to obtain. As discussed both in this section and in the following papers, such convergence is not expected until we have much more information on the geometry, the environment, the electronic structure and the binding in the given molecular junction. These issues of reliability are now being seriously addressed, and the field is making great progress toward turning molecular junction transport into a reliable model science.

Acknowledgements

Mark Ratner is grateful to the DoD MURI/DURINT program, the DARPA Moletronics/MOLEAPPS Program, the NSF-NCN program at Purdue University and the NASA URETI program for support of his work. AN thanks the Israel Science Foundation, the U.S. – Israel Binational Science Foundation and the Volkswagen Foundation for financial support of his research.

References

1. C. Joachim, J.K. Gimzewski, and A. Aviram: Electronics using hybrid-molecular and mono-molecular devices, *Nature* **408,** 541 (2000).
2. A. Nitzan and M. Ratner: Electron transport in molecular wire junctions, *Science* **300,** 1384 (2003).
3. A. Nitzan: Electron transmission through molecules and molecular interfaces, *Ann. Rev. Phys. Chem.* **52,** 681 (2001).
4. P. Hanggi, M. Ratner, and S. Yaliraki, eds., *Chemical Physics* **281,** 111 (2002).
5. J.R. Heath and M.A. Ratner: Molecular electronics, *Physics Today* 56, 43 (2003); C.R. Kagan and M.A. Ratner, eds., *MRS Bulletin*, **29**, #6 (2004)
6. D.M. Adams, L. Brus, C.E.D. Chidsey, et al.: Charge transfer on the nanoscale: Current status, *J. Phys. Chem. B* **107**, 6668 (2003).
7. M.C. Petty, M.R. Bryce, and D. Bloor, *Introduction to Molecular Electronics* (Oxford University Press, Oxford, 1995); C.A. Mirkin, and M.A. Ratner: Molecular electronics, *Annu. Rev. Phys. Chem.*, **43**, 719 (1992); A. Aviram, ed., *Molecular Electronics – Science and Technology* (American Institute of Physics, College Park, MD, 1992); A. Aviram, M.A. Ratner, and V. Mujica: Molecular electronics – science and technology, eds., *Ann. N.Y. Acad. Sci.,* **852**, (1998); J. Jortner, and M.A. Ratner, eds. *Molecular Electronics* (Blackwell Science, Cambridge, MA, 1997); M.A. Ratner, and M.A. Reed, *Encyclopedia of Science and Technology, 3rd ed.*, (Academic Press, New York, 2002); V. Mujica, and M.A. Ratner, in *Handbook of Nanoscience, Engineering and Technology*, W.A. Goddard III, D.W. Brenner, S.E. Lyshevshi, and G.J. Iafrate, eds. (CRC Press, Boca Raton, FL, 2002); M.A. Reed, and T. Lee, eds., *Molecular Nanoelectronics* (American Scientific Publishers, Stevenson Ranch, CA, 2003).
8. Jeffrey R. Reimers, et al.: Molecular Electronics III, eds., *Ann. N.Y. Acad. Sci.*, **1006**, (2003).
9. Thomas Tsakalakos, Ilya A. Ovid'ko and Asuri K. Vasudevan, eds., *Nanostructures: Synthesis, Functional Properties and Applications*, (Kluwer, Dordrecht, 2003).
10. A. Aviram, M. Ratner, and V. Mujica, eds., *Molecular electronics II, Ann. N.Y. Acad. Sci.*, **960,** (2002).
11. J. Jortner, and M. Bixon, in *Advances in Chemical Physics*, I. Prigogine, and S. Rice, eds. 106 (Wiley, New York, 1999); A.M. Kuznetsov, *Charge Transfer in Physics, Chemistry and Biology* (Gordon & Breach, New York, 1995); A.M. Kuznetsov, J. Ulstrup, A.M.K., et al., *Electron Transfer in Chemistry and Biology: An Introduction to the Theory* (Wiley, New York, 1998).
12. R.A. Marcus: Chemical and electrochemical electron-transfer theory, *Ann. Rev. Phys. Chem.* **15**, 155 (1964).
13. J.R. Miller, J.V. Beitz, and R. Huddleston: Effect of free energy on rates of electron transfer between molecules, *J. Am. Chem. Soc.* **106**, 5057 (1984).
14. J. Jortner and B. Pullman, eds., Perspectives in Photosynthesis. Dordrecht: Kluwer, 1990.
15. J. Jortner, M. Bixon, T. Langenbacher, and M.E. Michel-Beyerle: Charge transfer and transport in DNA, Proceed. *Natl. Acad. Sci. USA* **95**, 12759 (1998).
16. M. Bixon and J. Jortner, [1], p. 35.

17. J. Ulstrup and J. Jortner: The effect of intramolecular quantum modes on free energy relationships for electron transfer reaction, *J. Chem. Phys.* **63**, 4358 (1975).
18. M. Bixon and J. Jortner: Solvent relaxation dynamics and electron transfer, *Chem. Phys.* **176**, 467 (1993).
19. T. Holstein: Polaron motion. I. Molecular crystal model, *Ann. Phys. (N.Y.)* **8**, 325, 343 (1959).
20. H. McConnell: Intramolecular charge transfer in aromatic free radicals, *J. Chem. Phys.* **35**, 508 (1961).
21. J. Jortner: Temperature dependent activation energy for electron transfer between biological molecules, *J. Chem. Phys.* **64**, 4860 (1976); V. Mujca, M. Kemp, M. Roitberg, and M.A. Ratner: Electron conduction in molecular wires. I. A scattering formalism and II. Application to scanning tunneling microscopy, *J. Chem. Phys.* **101**, 6849, 6856 (1994).
22. J. Tersoff, and D.R. Hamann: Theory of the scanning tunneling microscope, *Phys. Rev. B*, **31**, 805 (1985).
23. R. Landauer: Spatial variation of currents and field due to localized scatterers in metallic conduction, *IBM J. Res. Dev.* **1**, 223, (1957); R. Landauer: Electrical resistance of disordered one-dimensional lattices, *Phil. Mag.,* **21**, 863 (1970).
24. C.W.J. Beenakker, and H. van Houten: Advances in research and applications. Qantum transport in semiconductor nanostructures, *Solid State Physics*, **44**, 1 (Academic Press, New York, 1991).
25. L.V. Keldysh, *Sov. Phys. JETP*, **20**, 1018 (1965).
26. L. P. Kadanoff, and G. Baym, *Quantum Statistical Mechanics; Green's function Methods in Equilibrium and Nonequilibrium* (W.A. Benjamin, New York, 1962).
27. Y. Meir and N.S. Wingreen: Landauer formula for the current through an interacting electron region, *Phys. Rev. Lett.* **68**, 2512 (1992)
28. T. Seideman, and W.H. Miller: Quantum mechanical reaction probabilities via a discrete variable representation-absorbing boundary condition Green's function, *J. Chem. Phys.*, **97**, 2499 (1992); T. Seideman, and W.H. Miller: Calculation of the cumulative reaction probability via a discrete variable representation with absorbing boundary conditions, *J. Chem. Phys*, **96**, 4412 (1992).
29. S. Datta, *Electric transport in Mesoscopic Systems* (Cambridge University Press, Cambridge, 1995); S. Datta, to be published.
30. Y. Xue, S. Datta, and M.A. Ratner: Charge transfer and "band lineup" in molecular electronic devices: A chemical and numerical interpretation, *J. Chem. Phys.*, **115**, 4292 (2001).
31. L.E. Hall, J.R. Reimers, N.S. Hush, et al.: Formalism, analytical model, and a priori Green's-function-based calculations of the current-voltage characteristics of molecular wires, *J. Chem. Phys.*, **112**, 1510 (2000).
32. S. Datta, W.D. Tian, S.H. Hong, et al.: Current-voltage characteristics of self-assembled monolayers by scanning tunneling microscopy, *Phys. Rev. Lett.*, **79**, 2530 (1997).
33. H. Ness, and A.J. Fisher: Quantum inelastic conductance through molecular wires, *Phys. Rev. Lett.*, **83**, 452 (1999); E.G. Petrov, I.S. Tolokh, and V. May: The magnetic-field influence on the inelastic electron tunnel current mediated

by a molecular wire, *J. Chem. Phys.*, **109**, 9561 (1998); E.G. Emberly, and G. Kirczenow: Electron standing-wave formation in atomic wires, *Phys. Rev. B*, **60**, 6028 (1999); E.G. Emberly, and G. Kirczenow: Models of electron transport through organic molecular monolayers self-assembled on nanoscale metallic contacts, *Phys. Rev. B*, **64**, 235412 (2001); M. Brandbyge et al.: Density-functional method for nonequilibrium electron transport, *Phys. Rev. B*, **65**, 165401 (2002); B. Larade, et al.: Conductance, *I-V* curves, and negative differential resistance of carbon atomic wires, *Phys. Rev. B*, **64**, 075420 (2001); J. Taylor, H. Guo, J. Wang: Ab initio modeling of open systems: Charge transfer, electron conduction, and molecular switching of a C_{60} device, *Phys. Rev. B*, **63**, 121104(R) (2001); M. Magoga, and C. Joachim: Minimal attenuation for tunneling through a molecular wire, *Phys. Rev. B*, **57**, 1820 (1998); M. Magoga, and C. Joachim: Conductance of molecular wires connected or bonded in parallel, *Phys. Rev. B*, **59**, 16011 (1999); P. Stampfus, et al., in *Proceedings NIC Symposium*; D. Wolf, G. Munster, M. Kremer, eds., **20**, 101 (2003); R. Baer and D. Neuhauser: Ab initio electrical conductance of a molecular wire, *Int. J. Quant. Chem.*, **91**, 524 (2003); R. Baer, et al: Ab initio study of the alternating current impedance of a molecular junction, *J. Chem. Phys.* **120**, 3387 (2004).

34. J.K. Tomfohr, and O. Sankey: Complex band structure, decay lengthg, and Fermi level alignment in simple molecular electronic systems, *Phys. Rev. B*, **65**, 245105 (2002); B. Larade, J. Taylor, H. Mehrez, and H. Guo: Conductance, *I-V* curves, and negative differential resistance of carbon atomic wires, *Phys Rev. B*, **64**, 075420 (2001); J. Taylor, H. Guo, and J. Wang: Ab initio modeling of open systems; Charge transfer, electron conduction, and molecular switching of a C_{60} device, *Phys. Rev. B*, **63**, 121104(R) (2001); H. Mehrez, G. Hong, J. Wang, and C. Roland: Carbon nanotubes in the Coulomb blockade regime, *Phys. Rev. B*, **63**, 245410/1 (2001); A. di Carlo et al.: Theoretical tools for transport in molecular nanostructures, Physica B, **314**, 86 (2002); J.C. Cuevas et al.: theoretical description of the electrical conduction in atomic and molecular junctions, Nanotechnology, **14**, R29 (2003); J.J. Palacios et al.: First-principal approach to electrical transport in atomic-scale nanostructures, Phys. Rev. B**, 66**, 035322 (2002).
35. Y.Q. Xue and M.A. Ratner: Microscopic study of electrical transport through individual molecules with metallic contacts. (2). Effect fo the interface structure, *Phys. Rev. B,* **68**, 115407 (2003); and: Schottky barrier at metal-finite semiconduction carbon nanotube interfaces, *Appl. Phys. Lett.* **83**, 2429 (2003).
36. T. Seideman, and H. Guo: Quantum transport and current-triggered dynamics in molecular tunnel junctions, *J. Theor. Comp. Chem.*, **2**, 439 (2004).
37. N.D. Lang: Resistance of atomic wires, *Phys. Rev. B*, **52**, 5335 (1995).
38. N.D. Lang, and P. Avouris: Carbon-atom wires: Charge-transfer doping, voltage drop, and the effect of distortions, *Phys. Rev. Lett.*, **84**, 358 (2000).
39. M. diVentra, S. Pantelides, and N. Lang: Erratum: Current-induced forces in molecular wires [Phys. Rev. Lett., **88**, 046801 (2002)], *Phys. Rev. Lett.*, **89**, 139902 (2002); M. Di Ventra, and S.T. Pantelides: Scanning tunneling microscopy images: A full ab initio approach, *Phys. Rev. B*, **59**, R5320 (1999).
40. S.N. Rashkeev, M. Di Ventra, and S.T. Pantelides: Transport in molecular transistors: Symmetry effects and nonlinearities, *Phys. Rev. B*, **66**, 033301/1 (2002); Y. Zhongqin, N.D. Lang, and M. Di Ventra: Effects of geometry and

doping on the operation of molecular transistors, *App. Phys. Lett.*, **82**, 1938 (2003); S.T. Pantelides, M. Di Ventra, and N.D. Lang: First-principles simulations of molecular electronics, *Ann. N.Y. Acad. Sci.,* **960**, 177 (2002); S.T. Pantelides, M. Di Ventra, N.D. Lang, and S.N. Rashkeev: Molecular electronics by the numbers, *IEEE Transactions on Nanotechnology*, **1**, 86 (2002); M. Di Ventra, N.D. Lang, and S.T. Pantelides: Electronic transport in single molecules, *Chem. Phys.*, **281**, 189 (2002); M. Di Ventra, S.T. Pantelides, and N.D. Lang: Current-induced forces in molecular wires, *Phys. Rev. Lett.*, **88**, 046801 (2002); M. Di Ventra, and N.D. Lang: Transport in nanoscale conductors from first principles, *Phys. Rev. B*, **65**, 045402 (2002).

41. A. Troisi, and M.A. Ratner: Molecular wires conductance: Some theoretical and computational aspects, *Molecular Nanoelectronics*, M.A. Reed, and T. Lee, eds., 1 (American Scientific Publishers, Stevenson Ranch, CA, 2003).
42. R.H.M. Smit, Y. Noat, C. Untiedt, N.D. Lang, M.C.V. Hemert, and J.M. van Ruitenbeek: Measurement of the conductance of a hydrogen molecule, *Nature*, **419**, 906 (2002).
43. M. Fuhrer, S.A. Getty, L. Wang, C. Engtrakul, and L. R. Sita: Near-perfect conduction through a ferrocene-based molecular wire, unpublished.
44. A. Nitzan: A relationship between electron-transfer rates and molecular conduction, *J. Phys. Chem. A*, **105**, 2677 (2001).
45. A. Nitzan: The relationship between electron-transfer rate and molecular conduction. (2). The sequential hopping case, *Israel J. Chem.,* **42**, 163 (2002).
46. R.A. Marcus: On the theory of electron-transfer reactions. (6). Unified treatment for homogeneous and electrode reactions, *J. Chem. Phys.*, **43**, 679 (1965); M.D. Newton: Quantum chemical probes of electron-transfer kinetics: The nature of donor acceptor interactions, *Chem. Rev.*, **91**, 767 (1991).
47. D.M. Adams et al.: Charge transfer on the nanoscale: Current status, *J. Phys. Chem. B,* **107**, 6668 (2003)
48. J. Park, A.N. Pasupathy, J.I. Goldsmith, C.C. Chang, Y. Yaish, J.R. Petta, M. Rinkoski, J.P. Sethna, H.D. Abruna, P.L. McEuen, and D.C. Ralph: Coulomb blockade and the Kondo effect in single-atom transistors, *Nature*, **417**, 722 (2002); W. Liang et al.: Kondo resonance in a single-molecule transistor, *Nature* **417**, 725 (2002)
49. S. Kubatkin, A. Danilov, M. Hjort, J. Cornil, J.-L. Bredas, N. Stuhr-Hansen, P. Hedegard, and T. Bjornholm: Single-electron transistor of a single organic molecule with access to several redox states, *Nature*, **425**, 698 (2003).
50. D. Segal and A. Nitzan: Steady-state quantum mechanics of thermally relaxing systems, *Chem. Phys.* 268, 315 (2001); D. Segal, and A. Nitzan: Heating in current carrying molecular junctions, *J. Chem. Phys.*, **117**, 3915 (2002).
51. D. Segal, A. Nitzan, and P. Hanggi: Thermal conductance through molecular wires, *J. Chem. Phys.*, **119**, 6840 (2003).
52. Y.-C. Chen, M. Zwolak, and M. DiVentra: Local heating in nanoscale conductors, *Nano Lett.*, **3**, 1691 (2003); T.N. Todorov: Local heating in ballistic atomic-scale contacts, *Philosoph. Mag. B*, **77**(4), 965 (1998); M.J. Montgomery, T.N. Todorov, and A.P. Sutton: Power dissipation in nanoscale conductors, *J. Phys.: Cond. Matt.*, **14**, 5377 (2002).
53. B.C. Stipe, M.A. Rezaei, and W. Ho: Inducing and viewing the rotational motion of a single molecule, *Science*, **279**, 1907 (1998).

54. B.C. Stipe, M.A. Rezaei, and W. Ho: Localiztion of inelastic tunneling and the determination of atomic-scale structure with chemical specifity, *Phys. Rev. Lett.*, **82**, 1724 (1999).
55. T. Komeda, Y. Kim, M. Kawai, B.N.J. Persson, and H. Ueba: Lateral hopping of molecules induced by excitation of internal vibration mode, *Science*, **295**, 2055 (2002).
56. S. Alavi, B. Larade, J. Taylor, H. Guo, and T. Seideman: Current-triggered vibrational excitation in single-molecule transistors, *Chem. Phys.*, **281**, 293 (2002); T. Seideman: Current-triggered dynamics in molecular-scale devices, *J. Phys.: Cond. Matt.*, **15**, R521 (2003); B.N.J. Persson, and H. Ueba; Theory of inelastic tunneling induced motion of adsorbates on metal surfaces, *Surf. Sci.*, **12**, 502 (2002).
57. S.-W. Hla, L. Bartels, G. Meyer, and K.-H. Rieder: Inducing all steps of a chemical reaction with the scanning tunneling microscope tip: Towards single molecule engineering, *Phys. Rev. Lett.*, **85**, 2777 (2000); G.V. Nazin, X.H. Qiu, and W. Ho: Visualization and spectroscopy of a metal-molecule-metal bridge, *Science*, **302**, 77 (2003); J.R. Hahn, and W. Ho: Oxidation of a single carbon monoxide molecule manipulated and induced with a scanning tunneling microscope, *Phys. Rev. Lett.*, **87**, 166102 (2001).
58. E.L. Wolf, *Principles of electron tunneling spectroscopy* (Oxford University Press, New York, 1985); K.W. Hipps and U. Mazur: Inelastic electron tunneling: An alternative molecular spectroscopy, *J. Phys. Chem.*, **97**, 7803 (1993).
59. H.J. Lee and W. Ho: Single-bond formation and characterization with a scanning tunneling microscope, *Science*, **286**, 1719 (1999); N. Lorente, M. Persson, L.J. Lauhon, and W. Ho: Symmetry selection rules for vibrationally inelastic tunneling, *Phys. Rev. Lett.*, **86**, 2593 (2001); J.R. Hahn, and W. Ho: Single molecule imaging and vibrational spectroscopy with a chemical modified tip of a scanning tunneling microscope, *Phys. Rev. Lett.*, **87**, 196102 (2001); L.J. Lauhon and W. Ho: Direct observation of the quantum tunneling of single hydrogen atoms with a scanning tunneling microscope, *Phys. Rev. Lett.*, **85**, 4566 (2000); J. Gaudioso, J.L. Laudon, and W. Ho: Vibrationally mediated negative differential resistance in a single molecule, *Phys. Rev. Lett.*, **85**, 1918 (2000); L.J. Lauhon and W. Ho: Single-electron vibrational spectroscopy and microscopy: CO on Cu(001) and Cu(110), *Phys. Rev. B*, **60**, R8525 (1999); H.J. Lee and W. Ho: Structural determination by single-molecule vibrational spectroscopy and microscopy: Contrast between copper and iron carbonyls, *Phys. Rev. B*, **61**, R16347 (2000).
60. J.R. Hahn, H.J. Lee, and W. Ho: Electronic resonance and symmetry in single-molecule inelastic electron tunneling, *Phys. Rev. Lett.*, **85**, 1914 (2000).
61. N.B. Zhitenev, H. Meng, and Z. Bao: Conductance of small molecular junctions, *Phys. Rev. Lett.*, **88**, 226801 (2002); H. Park, J. Park, A.K.L. Lim, E.H. Anderson, A.P. Alivisatos, and P.L. McEuen: Nanomechanical oscillations in a single-C_{60} transistor, *Nature*, **407**, 57 (2000).
62. W. Wang, T. Lee, I. Kretzschmar, and M.A. Reed: Inelastic electron tunneling spectroscopy of alkanedithiol self-assembled monolayers, *Nano Lett.*, **4**, 643 (2004); J.G. Kushmerick, J. Lazorcik, C.H. Patterson, R. Shashidhar, D.S. Seferos, and G.C. Bazan: Vibronic contributions to charge transport across molecular junctions, *Nano Lett.*, **4**, 639 (2004).

63. A. Nitzan, M. Galperin, and M.A. Ratner: Inelastic electron tunneling spectroscopy in molecular junctions: Peaks and dips, submitted for publication (cond-mat/0405472).
64. A. Nitzan, J. Jortner, J. Wilkie, et al.: Tunneling time for electron transfer reactions, *J. Phys. Chem. B*, **104**, 5661-5665 (2000).
65. U. Peskin, A. Edlund, I. Bar-On, et al.: Transient resonance structures in electron tunneling through water, *J. Chem. Phys.*, **111**, 7558 (1999).
66. E. Yablonovitch: The chemistry of solid-state electronics, *Science*, **246**, 347 (1989).
67. R. Venugopal, M. Paulsson, S. Goasguen, S. Datta, and M. Lundstrom: A simple quantum mechanical treatment of scattering in nanoscale transistors, *J. App. Phys.*, **93**, 5613 (2003); M. Buttiker: Four-terminal phase-coherent conductance, *Phys. Rev. Lett.,* **57**, 1761 (1986).
68. M. Bixon, and J. Jortner: Vibrational coherence in nonadiabatical dynamics, *J. Chem. Phys.*, **107**, 1470 (1997).
69. M. Bixon, and J. Jortner: Electron transfer via bridges, *J. Chem. Phys.*, **107**, 5154 (1997).
70. Y. Selzer, et al.: Temperature effects on conduction through a molecular junction, Nanotechnology 15, S483 (2004); and: Thermally activated conduction in molecular junctions, J. Am. Chem. Soc. **126,** 4052 (2004).
71. B. Giese et al.: Direct observation of the hole transfer through DNA by hopping between adenine beaes and by tunneling, *Nature* **412**, 318 (2001).
72. D. Segal, A. Nitzan, W.B. Davis, M.R. Wasilewski, and M.A. Ratner: Electron transfer rates in bridged molecular systems. 2. A steady-state analysis of coherent tunneling and thermal transitions, *J. Phys. Chem. B*, **104**, 3817 (2000); D. Segal, and A. Nitzan: Conduction in molecular junctions: Inelastic effects, *Chem. Phys.*, **281**, 235 (2002); D. Segal, and A. Nitzan: Steady-state quantum mechanics of thermally relaxing systems, *Chem. Phys.*, **268**, 315 (2001), and references therein.
73. D. Segal, and A. Nitzan: Heating in current carrying molecular junctions, *J. Chem. Phys.*, **117**, 3915 (2002).
74. X.H. Qiu, G.V. Nazin, and W. Ho: Vibronic states in single molecule electron transport, *Phys. Rev. Lett.*, **92**, 206102 (2004).
75. B.N.J. Persson, and A. Baratoff: Inelastic electron tunneling from a metal tip: The contribution from resonant processes, *Phys. Rev. Lett.*, **59**, 339 (1987).
76. A. Bayman, P. Hansma, and W.C. Kaska: Shifts and dips in inelastic-electron-tunneling spectra due to the tunnel-junction environment, *Phys. Rev. B*, **24**, 2449 (1981).
77. M. Galperin, M.A. Ratner, and A. Nitzan: Hysteresis, switching and negative differential reistance in molecular junctions: A polaron model, Nano Letters, **5**(1), 125 (2005).
78. M.R. Wasielewski: Photoinduced electron transfer in supramolecular systems for artificial photosynthesis, *Chem. Rev.*, **92**, 435 (1992).
79. G. Closs, J.R. Miller: Intramolecular long-distance electron transfer in organic molecules, *Science*, **240**, 440 (1988).
80. J. Lehmann, S. Kohler, P. Hanggi, and A. Nitzan: Molecular wires acting as coherent quantum ratchets, *Phys. Rev. Lett.*, **88**, 228305 (2002); J. Lehmann, S. Kohler, P. Hanggi, and A. Nitzan: Rectification of laser-induced eletronic transport through molecules, *J. Chem. Phys.*, **118**, 3283 (2002); S. Kohler,

S. Camalet, M. Strass, J. Lehmann, G.-L. Ingold, and P. Hanggi: Charge transport through a molecule driven by a high-frequency field, *Chem. Phys.*, **296**, 243 (2004); J. Lehmann, S. Camalet, S. Kohler, and P. Hanggi: Laser controlled molecular switches and transistors, *Chem. Phys. Lett.*, **368**, 282 (2003); A. Keller, O. Atabek, M. Ratner, and V. Mujica: Laser-assisted conductance of molecular wires, *J. Phys. B Atomic Molecular & Optical Physics*, **35**, 4981 (2002); A. Tikhonov, R.D. Coalson, and Y. Dahnovsky: Calculating electron transport in a tight-binding model of a field driven molecular wire: Floquet theory, *J. Chem. Phys.*, **116**, 10909 (2002); A. Tikhonov, R.D. Coalson, and Y. Dahnovsky: Calculating electron current in a tight-binding model of a field driven molecular wire: Application to xylyl-dithiol, *J. Chem. Phys.*, **117**, 567 (2002).

81. Y. Kamada, N. Naka, S. Saito, N. Nagasawa, Z.M. Li, and Z.K. Tang: Photoirradiation effects on electrical conduction of single wall carbon nanotubes, *Solid State Communications*, **123**, 375 (2002); V. Gerstner, A. Knoll, W. Pfeiffer, A. Thon, and G. Gerber: Femtosecond laser assisted scanning tunneling microscopy, *J. Appl. Phys.*, **88**, 4851 (2000); R.J. Schoelkopf, A.A. Kozhevnikov, D.E. Prober, and M.J. Rooks: Observation of "photon-assisted" shot-noise in a phase-coherent conductor, *Phys. Rev. Lett.*, **80**, 2437 (1998); R.J. Schoelkopf, P.J.B. , A.A. Kozhevnikov, D.E. Prober, and M.J. Rooks: Frequency dependence of shot noise in a diffusive mesoscopic conductor, *Phys. Rev. Lett.*, **78**, 3370 (1997); B.J. Keay, S.J. Allen, Jr., J. Galán, J.P. Kaminski, K.L. Campman, A.C. Gossard, U. Bhattacharya, and M.J.W. Rodwell: Photon-assisted electric field domains and multiphoton-assisted tunneling in semiconductor superlattices, *Phys. Rev. Lett.*, **75**, 4098 (1995); Dulic D, et al.: One-way optoelectronic switching of photochromic molecules on gold, Phys. Rev. Lett., **91**, 207402 (2003).
82. T. Frauenheim, et al.: Atomistic simulations of complex materials: Ground state and excited-state properties, *J. Phys. Cond. Matt.*, **14**, 3015 (2002).
83. C.W. Bauschlicher, Jr., A. Ricca, Y. Xue, and M.A. Ratner: Current-voltage curves for molecular junctions: pyrene versus diphenylacetylene, *Chem. Phys. Lett.*, **390**, 246 (2004); J.M. Seminario, L.E. Cordova and P.A. Derosa: An ab initio approach to the calculation of current-voltage characteristics of programmable molecular devices, Proc. IEEE **91**, 1958 (2000); Y. Xue, S. Datta, and M.A. Ratner: Charge transfer and "band lineup" in molecular electronic devices: A chemical and numerical interpretation, *J. Chem. Phys.*, **115**, 4292 (2001).
84. K. Tagami, L. Wang, and M. Tsukada: Interface sensitivity in quantum transport through single molecules, *Nano Lett.,* **4**, 209 (2004); E. Emberly and G. Kirczenow: Molecular spintronics: Spin-dependent electron transport in molecular wires, *Chem. Phys.* **281**, 311(2002); E.G Petrov, I.S. Tolokh and V. May: Magnetic field control of an electron tunnel current through a molecular wire, *J. Chem. Phys.* **108**, 4386(1998).
85. Z.Q. Yang and M. Di Ventra: Nonlinear current-induced forces in Si atomic wires, *Phys. Rev. B* **67**, 161311 (2003).
86. X.-Y. Zhu: Charge transport at metal-molecule interfaces: A spectroscopic view, *J. Phys. Chem. B*, **108**, (2004).
87. S. Datta, W. Tian, S. Hong, R. Reifenberger, J.I. Henderson, C.P. Kubiak: Current-voltage characteristics of self-assembled monolayers by scanning tun-

nelling microscopy, *Phys. Rev. Lett.*, **79**, 2530 (1997); W. Tian, S. Datta, S. Hong, R. Reifenberger, J.I. Henderson, and C.P. Kubiak: Conductance spectra of molecular wires, *J. Chem. Phys.*, **109**, 2874 (1998); Y. Xue, S. Datta, S. Hong, R. Reifenberger, J.I. Henderson, and C.P. Kubiak: Negative differential resistance in the scanning tunneling spectroscopy of organic molecules, *Phys. Rev. B*, **59**, R7852 (1999).

88. V. Mujica, A.E. Roitberg and M. Ratner: Molecular wire conductance: Eloctrostatic potential spatial profile, *J. Chem. Phys.* **112**, 6834 (2000)
89. A. Xue, and M.A. Ratner: Microscopic study of electrical transport through individual molecules with metallic contacts. II. Effect of the interface structure, *Phys. Rev. B*, **68**, 115407 (2003).
90. C. Liang, A.W. Ghosh, M. Paulsson, S. Datta: Electrostatic potential profiles of molecular conductors, *Phys. Rev. B*, **69**, 115302 (2004).
91. M. Di Ventra, S.T. Pantelides, and N.D. Lang: The benzene molecule as a molecular resonant-tunneling transistor, *App. Phys. Lett.*, **76**, 3448 (2000).
92. A. Bachtold, et al.: Scanned probe microscopy of electronic transport in carbon nanotubes, *Phys. Rev. Lett.*, **84**, 6082 (2000).
93. Y. Karzazi, et al.: Influence of contact geometry and molecular derivatization on the interfacial interactions between gold and conjugated wires, *Chem. Phys. Lett.*, **387**, 502 (2004); H. Basch, and M.A. Ratner: Binding at molecule/gold transport interfaces. II. Orbitals and density of states, *J. Chem. Phys.*, **119**, 11943 (2003).
94. F. Zahid, M. Paulsson and S. Datta: Electrical conduction through molecules, in *Advanced Semiconductors and Organic Nanotechniques*, H. Morkoc, ed., (Academic Press, New York, 2003).
95. F. Zahid, M. Paulsson et al., to be published.
96. A. Rassolov, M.A. Ratner, and J.A. Pople: Semiempirical models for image eletrostatics. I. Bare external charge, *J. Chem. Phys.*, **114**, 2062 (2001).
97. V. Mujica, M. Kemp, and M.A. Ratner: Electron conduction in molecular wires. I. A scattering formalism and II. Application to scanning tunneling microscopy, *J. Chem. Phys.*, **101**, 6849, 6856 (1994).
98. D.S. Kosov: Schrödinger equation for current carrying states, J. Chem. Phys., **116**, 6368 (2002); J. Tomfohr, O. F. Sankey: Theoretical analysis of electron transport through organic molecules, *J. Chem. Phys.,* **120**, 1542 (2004); K. Thygesen et al., work in progress; R. Car, K. Burke, et al, work in progress.
99. J. Reichert, H.B. Weber, M. Mayor, H.V. Lohneysen: Low-temperature conductance measurements on single molecules, *Appl. Phys. Lett.*, **82**, 4137 (2003); J.O. Lee et al.: Electrical transport study of phenylene-based π-conjugated molecules in a three terminal geometry, Annals Of The New York Academy Of Sciences, **1006**, 122 (2003); D. Janes et al., to be published; M.A. Reed, et al.: Conductance of a molecular junction, *Science*, **278**, 252 (1997). The structure assumed here may be incorrect: e.g. P.L. Pugmire, M.J. Tarlov, R.D. van Zee: The structure of benzenedimethanethiol self-assembled monolayers on gold grown by solution and vapor techniques, Langmuir, **19**, 3720 (2003).
100. N.P. Guisinger, M.E. Greene, R. Basu, A.S. Baluch, M.C. Hersam: Room temperature negative differential resistance through individual organic molecules on silicon surfaces, *Nano Lett.*, **4**, 55 (2004).

101. X.P. Cao, R.J. Hamers: Silicon surfaces as electron acceptors: Dative bounding of amines with Si(001) and Si(111) surfaces, *J. Am Chem Soc* **123**, 10988 (2001); S.N. Patitsas et al.: Current-induced organic-silicon bond breaking: Consequences for molecular devices, *Surf. Sci.* **457,** L425 (2000)
102. J.G. Kushmerick, et al.: Understanding charge transport in molecular electronics, *Ann. NY Acad. Sci.* **1006**, 277 (2003)
103. X.D. Cui, et al.: Reproducible measurement of single-molecule conductivity, *Science*, **294**, 571(2001).
104. B. Mantooth, et al.: Cross-correlation image tracking for adsorbate analysis and drift correction, *Rev. Sci. Inst.*, **73**, 313 (2002).
105. R.P. Andres, et al.: "Coulomb staircase" at room temperature in a self-assembled molecular nanostructure, *Science* **272**, 1323 (1996); A. Dhirani, et al.: Self-assembled molecular rectifiers, *J. Chem. Phys.* **106**, 5249 (1997); R. McCreery, et al.: Molecular rectification and conductance swithing in carbon-based molecular junctions by structural rearrangement accompanying electron injection, *J. Am. Chem. Soc.* **125**, 10748 (2003); D.J. Wold, et al.: Distance dependence of electron tunneling through aelf-assembled monolayers measured by conducting probe atomic force microscopy: Unsaturated versus saturated molecular junctions, *J. Phys. Chem. B,* **106**, 2813 (2002)
106. C. Lin, and C.R. Kagan: Layer-by-layer growth of metal-metal bonded supramolecular thin films and its use in the fabrication of lateral nanoscale devices, *J. Am. Chem. Soc.*, **125**, 336 (2003).
107. Y. Selzer, et al.: Temperature effects on conduction through a molecular junction, *Nanotechnology*, **15**, S483 (2004).
108. H. Basch, and M.A. Ratner, unpublished.
109. G. Poirier: Characterization of organosulfur molecular monolayers on Au(111) using scanning tunneling microscopy, *Chem. Revs.*, **97**, 1117 (1997).
110. S. Liu, R. Maoz, J. Sagiv: Planned nanostructures of colloidal gold via self-assemply on hierarchically assembled organic bilayer template patterns with in-situ generated terminal amino functionality, *Nano Lett.*, **4**, 845 (2004).
111. X.Y. Xiao, B.Q. Xu, N.J. Tao: Measurement of single molecule conductance: Benzenedithiol and benzenedimethanethiol; *Nano Lett.*, **4**, 267 (2004).
112. W. Wang, T. Lee, and M.A. Reed: Mechanism of electron conduction in self-assembled alkanethiol monolayer devices, *Phys. Rev. B*, **68**, 035416 (2003).
113. J.W. Gadzuk and E.W. Plummer: Field emission energy distribution (FEED), *Revs. Mod. Phys.*, **45**, 487 (1973).
114. G.G. Fagas, A. Kambili and M. Elstner: Complex band structure: A method to determine the off-resonant electron transport in oligomers, *Chem. Phys. Lett.*, **389**, 268 (2004); V. Mujica, and M.A. Ratner: Current-voltage characteristics of tunneling molecular junctions for off-resonance injection, *Chem. Phys.*, **264**, 395 (2002).
115. W. Wang, T. Lee, and M.A. Reed: Intrinsic molecular electronic transport: Mechanisms and mehtods, *J. Phys. Chem. B*, in press.
116. C.C. Kaun, H. Guo: Resistance of alkanethiol molecular wires, *Nano Lett.*, **3**, 1521 (2003).
117. H. Basch, and M.A. Ratner: Binding at molecule/gold transport interfaces. V. Comparison of different metals and molecular bridges, submitted to *J. Chem. Phys.*
118. A. Salomon, et al.: Comparison of electronic transport measurements on organic molecules, *Adv. Mat.* **15**, 1881 (2003)

119. P.E. Kornilovitch, A.M. Bratkovsky, and R. S. Williams: Bistable molecular conductors with a field-switchable dipole group, *Phys. Rev. B*, **66**, 245413 (2002).
120. E.G. Emberly, and G. Kirczenow: The smallest molecular switch, *Phys. Rev. Lett.*, **91**, 188301 (2003).
121. A. Troisi, M.A. Ratner: Conformational molecular rectifiers, *Nano Lett.*, **4**, 591 (2004).
122. T. Rakshit, G.C. Liang, A. Ghosh, S. Datta: Silicon based molecular electronics, cond-mat/0305695 (2003), submitted to Phys. Rev. Lett.